Aus dem Neurowissenschaftlichen Forschungszentrum
der Medizinischen Fakultät Charité – Universitätsmedizin Berlin

DISSERTATION

The two-neuron microcircuit: An *in vitro* model for studying synapse formation and function

zur Erlangung des akademischen Grades
Doctor of Philosophy (PhD)
im Rahmen des
International Graduate program Medical Neuroscience

vorgelegt der Medizinischen Fakultät
Charité – Universitätsmedizin Berlin

von

Chia-Ling Chang
aus Taipeh, Taiwan
22.06.2014

Table of Contents

List of Figures

List of Tables

Abstract

Neural circuits are composed of mainly glutamatergic and GABAergic neurons, which operate excitation and inhibition signals in the central nervous system. Precise balance between excitation and inhibition through synapse connections is crucial for normal brain function. Development of synaptic connectivity is governed by both activity-independent and activity dependent mechanisms. It has been found that neuronal activity modulates GABAergic synapse formation and function using slice or mass cultures. However, it is difficult to dissect the contribution of intrinsic programs from extrinsic environmental effects in an intact network to this process. Here, we perform electrophysiological, pharmacological and morphological techniques from two-neuron microculture preparations of mouse hippocampal glutamatergic and GABAergic neurons to investigate the input and output of cells in a developing circuit. In our reduced preparation where extrinsic effects are minimal, we find that glutamatergic neurons show no change in output or input regardless of partner neuron cell type or neuronal activity level. In contrast, we find that glutamatergic input causes the GABAergic neuron to modify its output, by way of an increase in synapse formation and a decrease in synaptic release efficiency. These findings are consistent with GABAergic synapse maturation observed in many brain regions. Additionally, changes in GABAergic output are cell wide and not target cell specific. We also find that glutamatergic neuronal activity determined the AMPA receptor properties of synapses on the partner GABAergic neuron. All modifications of GABAergic input and output required activity of the glutamatergic neuron. As our system has reduced extrinsic factors, the changes we see in the GABAergic neuron due to glutamatergic input may reflect initiation of maturation programs that underlie the formation and function of *in vivo* neural circuits.

Zusammenfassung

Neuronale Netzwerke bestehen größtenteils aus glutamatergen und GABAergen Neuronen, die für exzitatorische und inhibitorische Signale im zentralen Nervensystem verantwortlich sind. Das präzise Wechselspiel zwischen Anregung und Inhibierung durch synaptische Verbindungen ist essentiell für ein normal funktionierendes Gehirn. Die Entwicklung dieser synaptischen Verbindungen wird sowohl von aktivitätsabhängigen wie –unabhängigen Mechanismen kontrolliert. Experimente in Schnitten und Massenkultur konnten zeigen, dass neuronale Aktivität die Bildung und Funktion von GABAergen Synapsen beeinflusst. Allerdings ist es schwierig in solch komplexen Netzwerken den Einfluss intrinsischer Programme von extrinsischen Effekten der Umgebung zu unterscheiden.

Um den Input und Output von Zellen in einem sich entwickelnden Netzwerk zu untersuchen, verwenden wir elektrophysiologische, pharmakologische und morphologische Methoden in einer Zwei-Neuronen-Mikrokultur aus glutamatergen und GABAergen Neuronen aus dem Hippocampus von Mäusen. In diesem reduzierten System, bei dem extrinsische Effekte minimiert sind, beobachten wir, dass glutamaterge Neuronen keine Veränderung in ihrem Input und Output zeigen, unabhängig von ihrem „Partnerneuron“ oder dem neuronalen Aktivtätslevel. Im Gegensatz dazu zeigen GABAerge Neuronen, die einen glutamatergen Input erhalten, einen veränderten Output: Die Synapsenbildung ist erhöht und die synaptische Freisetzungseffizienz ist reduziert. Gleiches fand man auch bei der Reifung von GABAergen Synapsen in vielen Gehirnregionen. Die Veränderungen im GABAergen Output sind außerdem unabhängig von der Zielzelle und betreffen alle Synapsen. Wir zeigen, dass die glutamaterge synaptische Aktivität die AMPA-Rezeptor-Eigenschaften des GABAergen Partnerneurons bestimmt. Alle Veränderungen am GABAergen Input und Output setzen Aktivität des glutamatergen Neurons voraus. Da in unserem System die extrinsischen Einflüsse reduziert sind, könnten die Veränderungen, die wir in GABAergen Neuronen beobachten, wenn sie glutamatergen Input erhalten, ein Reifungsprogramm widerspiegeln, das der Bildung und Funktion von Netzwerken *in vivo* zu Grunde liegt.

Chapter I

Introduction and Background

A. Central nervous system (CNS)

The function of the CNS is to integrate the information received from all part of the body for generating proper behaviors. The CNS comprises spinal cord and the brain, in which the brain performs the major functional part of the CNS. The brain contains two classes of cells, the neuron and the glial cell. Neurons process information by transducing signals through synaptic connections (Fig. IA.1) and glial cells have many functions including the support the function of neurons. In this thesis, I will put the focus on the physiology of neurons. Two main types of neurons, excitatory and inhibitory, operate distinct signals in the CNS. Precise balance between excitatory and inhibitory neuronal activities is critical for the normal brain function and it requires coordinated changes in the connection and function between these two types of neurons (Turrigiano and Nelson, 2004; Ramamoorthi and Lin, 2011). To study how synapses form and function between excitatory and inhibitory neurons is an important initial step towards understanding information processing of the nervous system.

B. Fast synaptic transmission

In the nervous system, the synapse is a subcellular structure located at the nerve terminal that enables communication between neurons by passing electrical or chemical signals through electrical or chemical synapse, respectively (Kandel and Siegelbaum, 2000). In the vertebrate nervous system, most neurons communicate to each other by chemical synapses (Fig. IA.1). Chemical synaptic transmission depends on the release of neurotransmitter from the presynaptic neuron. The presynaptic terminals contain synaptic vesicles, each of which is filled with specific types of neurotransmitter. The synaptic vesicles cluster at regions of the membrane called active zones, which are specialized for releasing transmitter. When the action potential (AP) generated from the presynaptic neuron that propagates down to the axonal terminal, Ca^{2+} enters the presynaptic terminal through voltage gated calcium channels at the active zone (Fig. IA.1). The increase in intracellular calcium concentration triggers vesicles to fuse with the presynaptic membrane and release their neurotransmitters into the synaptic cleft, a process called exocytosis. The neurotransmitter molecules diffuse across the synaptic cleft and bind to the specific

receptors on the postsynaptic neurons (Fig. IA.1). This in turn activates the postsynaptic neurotransmitter receptors. The resulting ion influx alters the membrane conductance and membrane potential, or causes long-term changes by the activation of signaling cascades. The change in membrane potential of the postsynaptic neuron is critical for generating a new AP in its axonal hillocks. In this manner, the information can be conveyed further to the next postsynaptic neuron through the release of neurotransmitters at the synapse.

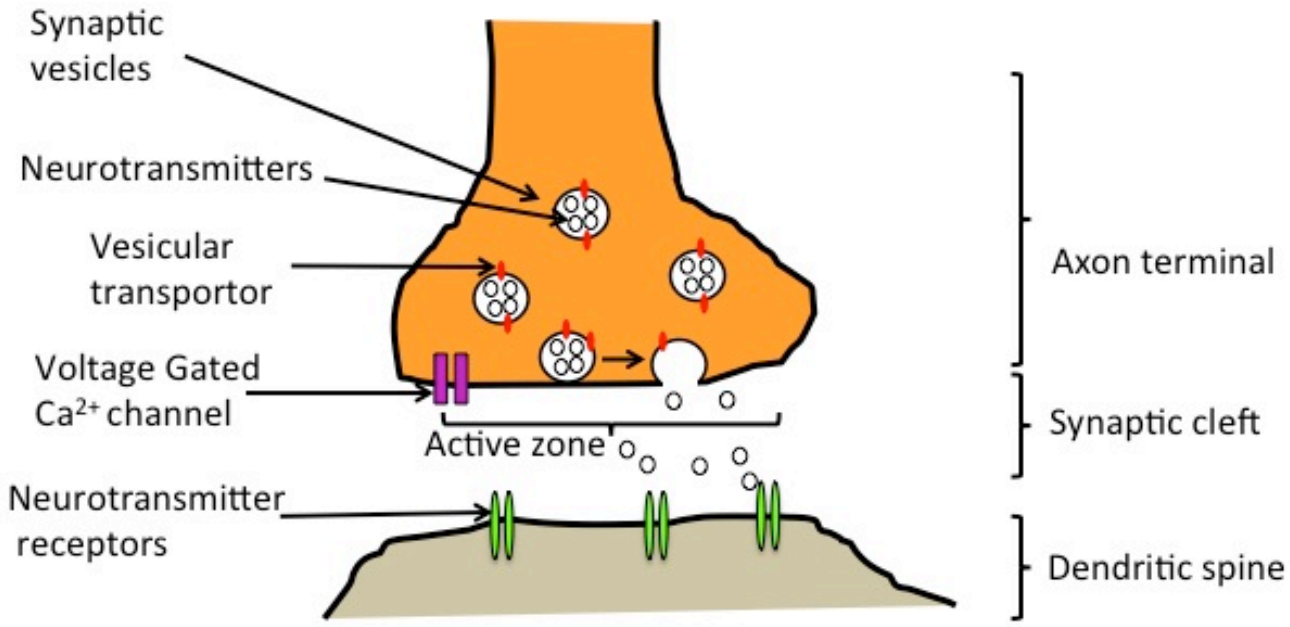

Figure IA.1 A diagram that illustrate the structure of a typical chemical synapse
The axon terminal from the presynaptic neuron contains neurotransmitters enclose in synaptic vesicles (SV). SV are docked at the presynaptic membrane at regions called active zones. To trigger the release of neurotransmitter, it requires the calcium influx through voltage gated Ca^{2+} channels at the axon terminal. Neurotransmitter receptors are located at the dendritic spine of the postsynaptic neuron. Between the pre- and the postsynaptic sites is a gap called the synaptic cleft.

C. Excitatory and inhibitory synaptic transmission

There are two types of chemical synapses that are responsible for excitatory and inhibitory neurotransmission. Excitatory and inhibitory signals are determined by the type of transmitter released from the presynaptic neurons and the type of ion channels gated by the transmitter on the postsynaptic neuron.

C1. Glutamatergic synapses

Glutamate is the primary excitatory neurotransmitter at most synapses in the CNS. Release of glutamate by glutamatergic neurons initiates excitatory neurotransmission. Before release, glutamate are actively taken up into synaptic vesicle (SV) by vesicular glutamate transporters (VGLUTs). Released glutamate binds to glutamatergic receptors such as AMPA (2-amino-3-(3-hydroxy-5-methyl-isoxazol-4-yl)propanoic acid) receptors. AMPA receptors are responsible for fast excitatory synaptic transmission in the CNS (Platt, 2007). Opening of AMPA receptors by glutamate conducts Na^+ and K^+ with nearly equal permeability. As a result, the reversal potential for current flow through these AMPA receptors is 0 mV. Therefore, opening of AMPA receptors will generate an inward current at the normal resting potential, which is around -65 mV, to depolarize the membrane potential.

In certain circumstance, AMPA receptor is also permeable Ca2+. The permeability of Ca^{2+} is determined by the expression of AMPA glutamate receptor 2 (GluA2) subunits. The AMPA receptor is a heteromultimetric structure comprised of glutamate subunits 1-4 (GluA1-4) (Hollmann and Heinemann, 1994; Traynelis et al., 2010). GluA2-containing AMPA receptors are not permeable to Ca^{2+}, which mostly observed in glutamatergic neurons in the CNS. However, GluA2-lacking AMPA receptors, which mostly observed in GABAergic neurons (Jonas et al., 1994; Geiger et al., 1995), are permeable to Ca^{2+} (Jonas and Burnashev, 1995). In addition, functional properties of GluA2-lacking AMPA receptors are modulated by membrane potential. Due to the channel blockade by intracellular polyamine at the positive membrane potential, current from GluA2-lacking AMPA receptor exhibits inward rectifying-current to voltage (I/V) relationship. This characteristic allows more inward than outward

current to pass through this receptor (McBain and Dingledine, 1993; Geiger et al., 1995; Isa et al., 1996).

The other type of ionotropic glutamate receptor is the NMDA (*N*-methyl-D-aspartate) receptor. NMDA receptors are permeable to Na^+, K^+ and Ca^{2+}. Unlike AMPA receptors, only glutamate is required to activate the opening of the receptor, the processes to activate NMDA receptors to open require the binding of glutamate and glycine as well as a depolarized membrane potential due to voltage dependent block of the channel by extracellular Mg2+ particularly at negative potentials.

C2. GABAergic synapse

Release of GABA (γ -aminobutyric acid) initiates inhibitory neurotransmission at the postsynaptic neuron. GABA is synthesized from glutamate by glutamic acid decarboxylase (GAD). Before release, GABA is actively taken up into vesicle by vesicular GABA transporter (VGAT). Released GABA binds to GABAergic receptors on the postsynaptic neurons. At ionotropic $GABA_A$ receptors, binding of GABA triggers the opening of a Cl^- selective channel pore. The increase Cl^- conductance drives the membrane potential towards the reverse potential of Cl^- ion, which is around -65 mV in neurons. Therefore, opening a GABA-gated channel will generate an outward current resulting predominantly in hyperpolarization of the postsynaptic neuron.

1. Synapse formation

The type of neurotransmitter it released in the synapse determines the type of presynaptic neuron. To match the presynaptic neurotransmitter release and postsynaptic response, it requires several developmental steps called synapse formation. Synapse formation involves the establishment of the selective connections between the tip of the growing axon, called the growth cone, and the dendrite as a first step (Fig. IA.1). In the second step, the growth cone differentiates into nerve terminal and the dendrite starts assembling postsynaptic proteins, including the proper postsynaptic receptors that match the neurotransmitter released. These steps are thought to depend on intercellular interactions that are largely governed by intrinsic genetic programs, such as molecules involve in axon guidance and cell-adhesion

complexes (Waites et al., 2005; Colon-Ramos, 2009; Lu et al., 2009). After forming the initial synaptic connections, synaptic transmission can begin. At the third step, properties and strength of the synapse is modulated by activity at the synapse. For example, during early development, spontaneous activity helps to establish the initial connectivity between neurons. During later development, sensory experience-dependent activity shapes postnatal circuit maturation (Katz and Shatz, 1996). As a result, the unused synapses will be eliminated and the useful synapses will be strengthened and stabilized (Cohen-Cory, 2002; Waites et al., 2005; Flavell and Greenberg, 2008). Therefore, development of synaptic connectivity is governed by both activity-independent and activity dependent mechanisms.

D1. Glutamatergic synapse formation

It has been suggested that neuronal activity-mediated release of glutamate modulates synapse formation, maturation and plasticity (Wong and Wong, 2001; Malinow and Malenka, 2002). Nevertheless, several evidences show that glutamatergic synapse formation is independent of neuronal activity *in vitro* (Rao and Craig, 1997; Verhage et al., 2000; Varoqueaux et al., 2002). For example, blocking neuronal activity by tetrodotoxin (TTX) in hippocampus mass cultures does not affect glutamatergic synapse formation (Rao and Craig, 1997). Munc13-1/Munc13-2 double knockout and Munc18-1 single knockout neurons show normal development of the glutamatergic synapses even if synaptic transmission is impaired in these mutant neurons (Varoqueaux et al., 2002). A recent study also shows that silencing of excitatory synaptic transmission on single neuron *in vivo* does not affect its synapse formation (Lu et al., 2013). These data suggest that glutamatergic neurons operate certain forms of synaptic formation in an activity independent manner. In addition, the number of glutamatergic synapse that a neuron can form is independent of the number of postsynaptic neurons (Harms et al., 2005). Taken together, these data suggest that glutamatergic neurons may operate hard-wire intrinsic mechanisms that govern initial glutamatergic synapse formation *in vitro*.

D2. GABAergic synapse formation

Neuronal activity promotes morphological maturation of the hippocampal GABAergic neuron *in vitro*. For example, neuronal activity increases GABAergic synapse number in hippocampal slices during postnatal weeks 1 to 3 (Marty et al., 2000; Colin-Le Brun et al., 2004; Marty et al., 2004). In visual and somatosensory cortex preparation, sensory deprivation during a critical postnatal period delays the maturation of GABAergic neuron innervations (Chattopadhyaya et al., 2004; Jiao et al., 2006). Furthermore, neuronal activity suppression by TTX leads to a decrease in the number GABAergic synapse number in the hippocampal mass culture (Hartman et al., 2006).

Neuronal activity mediated both trophic factor and neurotransmitter release, which is believed to modulate GABAergic synapse formation. Studies have been carried out to understand the cellular mechanisms that underlie activity-dependent GABAergic synapse formation. One of the mechanisms involved in this process is glutamatergic activity. For example, the GABAergic synapses require activity dependent release of brain-derived neurotrophic factor (BDNF) from the surrounding glutamatergic neurons (Goodman et al., 1996; Hartman et al., 2006; Park and Poo, 2013). BDNF is also shown to directly promote GABAergic synapse formation in the cultured cortical and hippocampal neurons (Rutherford et al., 1997; Vicario-Abejon et al., 1998; Marty et al., 2000; Palizvan et al., 2004). In addition to neurotrophic factors, spontaneous neuronal activity regulates GABAergic synapse formation (Chattopadhyaya et al., 2004; Colin-Le Brun et al., 2004). Spontaneous synaptic activities caused by the firing activity of cells through both glutamatergic and GABAergic receptors could modulate GABAergic synapse formation (Colin-Le Brun et al., 2004).

F. The strength of synaptic connections

The strength of signaling between two neurons depends on two main factors, synaptic strength and the number of synaptic connections they form. In the following paragraphs, I will highlight the essential components for synaptic strength and the strength of synaptic connections.

Synaptic strength is the product of vesicular release probability (P_{vr}), the size of the readily releasable pool (RRP) per synapse and the postsynaptic response to a vesicle release event (Q).

- **Synaptic strength = P_r (P_{vr} X RRP) X Q**
- **The strength of synaptic connections = synapse number X synaptic strength**

Release probability (P_r)

P_r is the likelihood of vesicle fusion and transmitter release occurring at a presynaptic terminal in response to an action potential (Del Castillo and Katz, 1954). P_r is correlated with the size of the RRP, synapses with a large RRP release vesicles with high probability than those with a smaller RRP (Dobrunz and Stevens, 1997; Dobrunz, 2002).

Vesicle release probability (P_{vr})

Vesicle release probability (P_{vr}) is defined as the likelihood that a single vesicle can be released upon an action potential (Zucker and Regehr, 2002). The average P_{vr} can be calculated by dividing the number of vesicle release due to action potential by the total number of readily releasable pool. P_{vr} plays an important role in presynaptic regulating short-term plasticity (Dobrunz and Stevens, 1997; Zucker and Regehr, 2002; Fioravante and Regehr, 2011) and is affected by microdomain [Ca^{2+}] (Neher and Sakaba, 2008) and the release machinery (Basu et al., 2007; Xue et al., 2008). The influence of [Ca^{2+}] microdomain on vesicle release is determined by the distance between the release sites to the calcium channels, the calcium buffer close to the Ca^{2+} channel and the amount of Ca^{2+} influx (Oheim et al., 2006). The modulation of calcium channels and calcium buffer is important for synaptic plasticity (Felmy et al., 2003). Furthermore, the synaptic release machinery also influences P_{vr}. For example, Complexin, an active zone protein, regulates vesicular release probability by directly acting on the molecular release machinery to enhance vesicle fusogenicity at glutamatergic and GABAergic neurons (Xue et al., 2008). Furthermore, phorbol ester

activation of C1 domain of Munc13-1 potentiates Ca^{2+} trigger release (higher P_{vr}) (Basu et al., 2007).

Overall, the synapses with initial high P_{vr} tend to show synaptic depression and synapses with initial low P_{vr} show synaptic facilitation (Dobrunz and Stevens, 1997). The degree of facilitation or depression of a synaptic connection can also be quantified by the paired-pulse ratio (PPR), which is defined as the amplitude ratio of the second to the first postsynaptic response after stimulation the connection with two action potentials (Zucker and Regehr, 2002). If the second response is larger than the first response which create a PPR larger than 1, this is called facilitation. If the second response is smaller than the first response, this is called depression where PPR is smaller than 1.

Readily releasable pool (RRP)

Neurotransmitters are stored in the vesicles that fuse with presynaptic plasma membrane upon action potential. The nerve terminal is packed with vesicles to sustain vesicle release during high frequency stimulation. A fraction of the total vesicle pool is close to the release site and is recruited first during synaptic activity. This population of vesicles is the readily releasable pool (RRP). The vesicles of RRP are fusion competent and can be released through action potential (Rizzoli and Betz, 2005). This pool contains about average 5 - 20 vesicles per synapses (Stevens and Tsujimoto, 1995; Rosenmund and Stevens, 1996; Rizzoli and Betz, 2005). The size of the RRP can be measured by application of hypertonic solution (Rosenmund and Stevens, 1996) or high frequency stimulation (Schneggenburger et al., 1999; Stevens and Williams, 2007). After release of vesicles, the RRP is supplied with vesicles from reserve pool.

Quantal size (Q)

Synaptic vesicle can be released spontaneously without action potential. This event generates miniature PSCs. The average amplitude of the postsynaptic response to the release of single vesicle is called quantal size. The quantal size can be measured as the amplitudes or charges of miniature excitatory postsynaptic currents

(mEPSCs) for vesicles filled with glutamate and miniature inhibitory postsynaptic currents (mIPSCs) for vesicles filled with GABA.

G. Homeostatic control of excitation and inhibition

A neuron in the CNS receives excitatory and inhibitory inputs from hundreds of neuron that determine its firing rate. Neuronal firing depends not only on the strength and number of the excitatory inputs but also inhibitory inputs (Mann and Paulsen, 2007). A precise balance between excitation and inhibition that a neuron receives is maintained within a proper range to avoid hyper- or hypo- excitation (Turrigiano and Nelson, 2004). To maintain this balance, it depends on several compensatory adjustments called homeostatic plasticity.

Homeostatic plasticity

Homeostatic plasticity is a negative-feedback response that neurons use to compensate hyper-excitation or hyper-inhibition in the brain circuitry. In order to stabilize neuronal excitability, synaptic and intrinsic properties of the neurons are homeostatic regulated (Turrigiano and Nelson, 2004; Turrigiano, 2007, 2011). Synaptic scaling is one of the best-characterized mechanisms of homeostatic plasticity (Turrigiano, 2008; Pozo and Goda, 2010). Synapse scaling regulates excitatory and inhibitory synapse strengths in response to changes in network activity in opposite directions (Turrigiano and Nelson, 2004). For example, globally blocking activity by voltage-gated sodium channel blocker tetrodotoxin (TTX) in hippocampal and cortical neuron cultures lead to scale up in the amplitudes of miniature excitatory postsynaptic currents (mEPSCs) (Turrigiano et al., 1998; Burrone et al., 2002). On the other hand, the miniature inhibitory postsynaptic currents (mIPSCs) onto pyramidal neurons are scaled down when neuronal activity is blocked (Kilman et al., 2002; Hartman et al., 2006). Furthermore, the postsynaptic receptors accumulation (Wierenga et al., 2005), the presynaptic release probability (Murthy et al., 2001; Thiagarajan et al., 2005; Wierenga et al., 2006; Turrigiano, 2007; Zhao et al., 2011) and intrinsic excitability (Burrone et al., 2002; Pratt and Aizenman, 2007; Turrigiano, 2007) also contribute to homeostatic readjustments of synaptic strength.

H. Deregulation of excitation and inhibition

A prerequisite for proper animal behavior is a balanced circuit (Turrigiano and Nelson, 2000; Klausberger and Somogyi, 2008; Shen et al., 2011; Yizhar et al., 2011). Aberrant excitatory/inhibitory neuronal activities and compensatory mechanisms lead to neurological disorders such as epilepsy (Noebels, 2003; Bozzi et al., 2013), Down syndrome (Fernandez and Garner 2007; Begenisic et al., 2011; Kleschevnikov et al., 2012) and Rett syndrome (Rubenstein and Merzenich, 2003; Zoghbi, 2003; Dani and Nelson, 2009; Kuzirian and Paradis, 2011).

Epilepsy

Epilepsy is a neurological disorders characterized by seizures (Chang and Lowenstein, 2003). Epilepsy is mostly caused from abnormal, hyper excitation of neuronal activity in the brain. One of many postulated mechanisms for epilepsy is the deregulation of inhibition levels through presynaptic reduction of GABA levels. This reduction of GABA levels is caused by mutation in glutamic acid decarboxylase (GAD), VGAT or postsynaptic receptors such as mutation in $GABA_A$ receptors (Noebels, 2003; Cobos et al., 2005).

Down syndrome

Down syndrome (DS) is caused from chromosome 21 trisomy (Lejeune et al., 1959). DS occurs in approximately 1 in 800 live birth (Roizen and Patterson 2003) and is characterized by attention and sensory deficits (Clark and Wilson, 2003). Several studies show that these cognitive deficits are resulted from excessive levels of inhibition in the brain (Baroncelli et al., 2011). For example, morphological changes in the inhibitory synapses such as enlargement of the active zones and increase of immunoreactivity for synaptic proteins such as GAD67 contribute to the increase of inhibitory synapse transmission (Belichenko et al., 2009; Perez-Cremades et al 2010). Furthermore, reducing inhibitory neurotransmission in DS mice model by $GABA_A$ receptor antagonist treatment enhances cognitive tasks (Fernandez et al., 2007).

Rett Syndrome

Rett syndrome (RTT) is a X-linked disease that results from mutations a single gene, *MeCP2* (Amir et al., 1999). *MeCP2* encodes for methyl-CpG binding protein-2, which functions as transcriptional activator and inhibitor (Chahrour et al., 2008). RTT occurs in approximately 1 in 10,000 female and is characterized by a 6-18 months normal developmental period followed by a series of neurological symptoms including seizure, tremor, mental retardation and autistic phenotype (Chahrour and Zoghbi, 2007). The function of MeCP2 in synapse development has been addressed experimentally in MeCP2- null as well as MeCP2-overexpressing mouse models (Chen et al., 2001; Guy et al., 2001; Collins et al., 2004). For example, MeCP2-null male mice show a decrease in glutamatergic synapse number while MeCP2-overexpressing mice show an increase in glutamatergic ysnapse number (Chao et al., 2007). A reduction in excitatory dendritic spine density has also been observed in MeCP2-null male mice (Belichenko et al., 2009; Tropea et al., 2009; Wood et al., 2009). Furthermore, there is a decrease in the excitation/inhibition ratio, which is due to hyper-inhibition in MeCP2-null male mice (Dani et al., 2005). This hyper-inhibition is partially due to reduced amplitude of mEPSCs without affecting the amplitude of mIPSCs in the MeCP2-null mice compared to wild type littermates (Dani and Nelson, 2009).

Furthermore, MeCP2 also regulates inhibition in the nervous system (Chao et al., 2010). Deletion of *MeCP2* specifically in GABAergic neurons decreases the amount of GABA by altering *Gad1/2* expression, leading to a reduced size of spontaneous miniature inhibitory postsynaptic currents (mIPSCs) (Chao et al., 2010). MeCP2-null mice also show changes in the strength and number of GABAergic synapses (Deng et al., 2010; Zhang et al., 2010). Mice with MeCP2 deficiency specifically in GABAergic neurons also display seizure phenotype (Chao et al., 2010). Taken together, these findings point out that maintenance of excitation and inhibition balance is critical for proper circuit function.

2. Aims

Precise balance of excitation-inhibition neuronal activity is crucial for proper brain function. This balance is determined by the pattern of synaptic connections and

how these synaptic connections behave. Forming the initial pattern of synaptic connections is largely governed by intrinsic mechanisms and is later refined by sensory input experience (Katz and Shatz, 1996). Because synaptic input and output function in early developing glutamatergic-GABAergic neural circuits set the foundation for a mature functional brain circuit, it is important to better understand how the basic circuit has been set up in the manner that largely independent of extrinsic factors. Therefore, in order to isolate the cell intrinsic mechanisms that govern synapse formation and function, we utilized an *in vitro* two-neuron microculture system where extrinsic factors are minimal.

There are three specific questions that we aim to address. First, we aimed to study how intrinsic mechanisms govern synapse formation and function by synaptic interaction between a glutamatergic and a GABAergic neuron. Second, we aimed to study whether the neuronal activity play a role in the modification of synapse formation and function during neuronal interaction. The first and the second aim will be addressed in Part A of Material and Methods, Results and Discussion. Third, we aimed to apply this system subsequently to identify the targets regulated by MeCP2 for glutamatergic synapse formation (see below, II.4). The third aim will be addressed in Part B of Material and Methods, Results and Discussion.

By understanding the general rules that govern glutamatergic and GABAergic synapse formation and function modulated by neuronal interaction, the result of this thesis may provide insights into how activity-dependent modulates excitation/inhibition coordination, which contributes to normal brain function. Furthermore, the application of this two-neuron microculture system to study the mechanisms of MeCP2 deficiency affecting the synaptic input/output of a neuron, we hoped to uncover the complexity of Rett syndrome mechanisms.

I. Experimental approach

I.1 Limitations of previous work

Several studies have suggested that neuronal activity regulates the GABAergic synaptic strength in the developing brain (Rutherford et al., 1997; Marty et al., 2000; Chattopadhyaya et al., 2004; Colin-Le Brun et al., 2004; Hartman et al., 2006). All of

these studies were performed in network-preserved systems such as mass cultures and slice cultures, where both intrinsic and extrinsic factors contribute to synapse formation and modulation. For example, global neuronal activity blockade by TTX in the hippocampal mass culture (Colin-Le Brun et al., 2004; Hartman et al., 2006) and slice culture (Marty et al., 2000) reduce in the number of GABAergic synapses. Interestingly, manipulation of activity in single pre or postsynaptic neuron in the mass culture failed to alter GABAergic synapse formation suggesting that GABAergic synapse formation requires the activity from surrounding neurons (Hartman et al., 2006). However, there are several limitations regarding to the network preparation in terms of technique and mechanistic function. First, it is difficult to control the input to the target neuron; therefore how input activity affects synapse formation and function of the target neuron is largely unknown. Second, the modulation of output functions of a neuron is difficult to measure since the output synapses are distributed to a heterogeneous population of neurons. Lastly, specific synapse formation and function are well controlled within neuronal circuits by a combination of cell autonomous and non-cell autonomous mechanisms during development (Craig and Boudin, 2001; Waites et al., 2005; Craig et al., 2006; Colon-Ramos, 2009; Huang, 2009; Lu et al., 2009). The degree to which synaptic function at an individual connection is established by neuronal activity and/or a set of specific pre- and postsynaptic molecular factors is largely unknown. Understanding the underlying control mechanism is difficult, as numerous cell intrinsic programs coexist with extrinsic mechanisms.

I2. Microculture

In order to better control the synaptic input and output properties and isolate intrinsic mechanisms that govern synapse formation and function, autaptic and two-neurons primary cultures were used in this dissertation.

a. Autaptic culture

A neuron sends its output signal (output) at the axonal terminal and receives the input signal (input) at the dendrite (Fig. II.2a-1). Autaptic culture is a well-studied model for understanding the synaptic properties (Bekkers and Stevens, 1991). In this preparation, a single neuron grown on a glial island forms synapses onto itself, so that

this neuron is both pre and post neuron (Figure II.2a-2b). There are several advantages of this culture system. First, the regulation of synaptic formation and function of an autaptic neuron is largely governed by intrinsic factors, which are difficult to dissect out from the network preparation. Second, it is a perfect system to quantify alterations in the morphology of a neuron, since the correlation of the morphology and the synaptic properties can be distinguished easily. Third, the axon of an autaptic neuron generates the synaptic output where input to its own dendrite. Therefore, the synaptic output is equal to synaptic input in autaptic circuit (Fig. II.2a-2a). The input/output function can be measured by single electrode with whole cell recording. In this dissertation, postsynaptic responses were used to measure of neurotransmitter release, which is determined by the probability of vesicle release, the number of readily releasable vesicle and the size of miniature postsynaptic response. The size of postsynaptic responses (Fig. II.2a-2c) and miniature postsynaptic responses can be measured by recording. The readily releasable vesicles can be depleted by hypertonic solution (Rosenmund and Stevens, 1996). The size of the readily releasable pool per neuron can be measured by applying hypertonic sucrose solution (Fig. II.2a-2d). P_{vr} is calculated as the ratio of the size of postsynaptic response and the size of RRP.

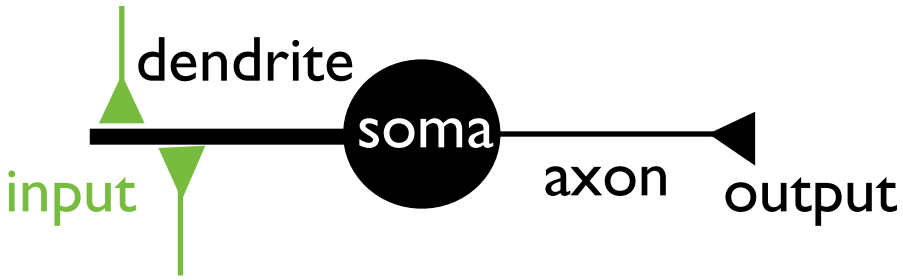

Figure II.2a-1 A diagram illustrates the synaptic input and output of a neuron.
A neuron sends synaptic output signal (black triangle) in the direction of soma to axonal terminal. The same neuron receives the synaptic input from the presynaptic terminal of the other neuron (green triangle) by activating receptors on the dendrite. The input signal then transmits in the direction to soma. The input signals from different inputs will be integrated at the axon initial segment to trigger action potential for generating its synaptic output.

a

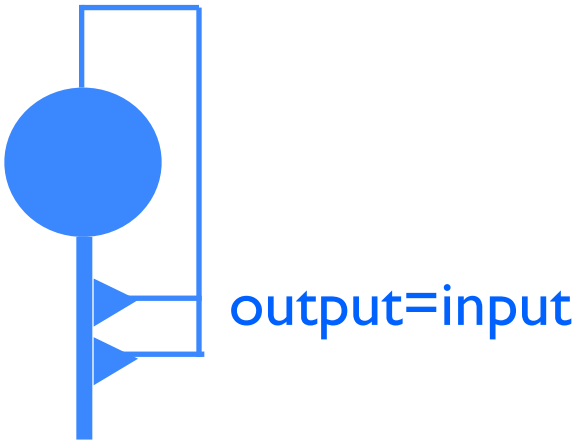

b

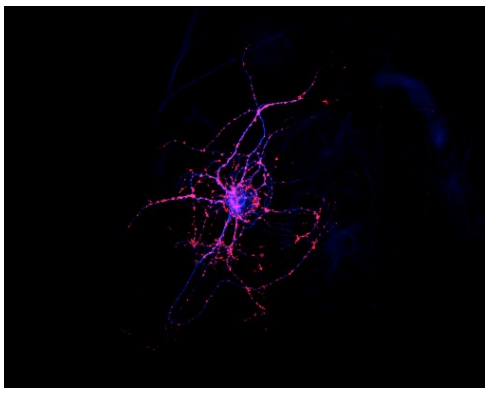

c

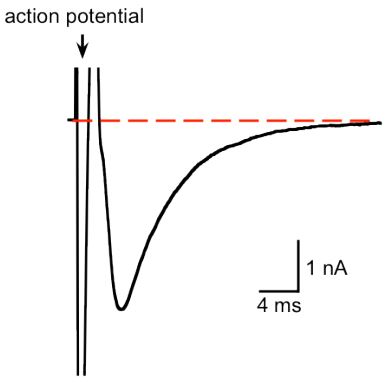

d

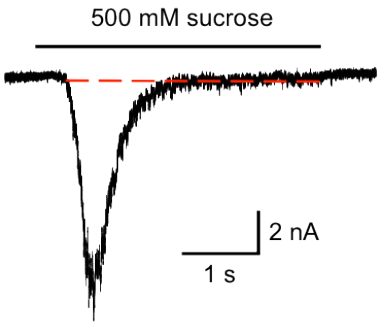

Figure II.2a-2 Diagrams illustrate the synaptic connections in a single neuron
(a) Cartoon diagrams illustrate single neuron forms autaptic connections by contacting its axon to dendrite. Therefore, the input response will be equal to the output response. (b) A single autaptic glutamatergic neuron grown on a glial island and labeled by vesicular glutamate transporter 1 (VGLUT1) and microtubule- associated protein 2 (MAP2). (c) An excitatory postsynaptic current (EPSC) from an autaptic neuron which is evoked by an action potential. (d) A postsynaptic response to 500 mM sucrose solution as the measurement of readily releasable pool size. (c, d) Vesicular release probability is calculated by dividing the charge of the EPSC (integral under the red dash line in **c**) to the charge of readily releasable pool (integral under the red dash line in **d**).

b. Two-neuron microculture

In this dissertation, I employed a two-neuron microculture system to study synapse formation and function governed by interaction between two neurons. Two-neuron microculture system preserves all the advantages from autaptic culture and also provides an ability to study the interaction between neurons. By providing better control of synaptic input and output of a neuron for studying synapse formation and function, we examined the properties of synaptic connections in homotypic (Fig. II.2b-1) and heterotypic (Fig. II.2b-2) pairs. Autaptic connection is defined as the synaptic connections onto itself. Heterosynaptic connection is defined as the synaptic connections onto the partner neuron. In paired neurons, a neuron forms autaptic as well as heterosynaptic connections (Fig. II.2b-1 and II.2b-2). In homotypic pairs of neurons, the synaptic connections from a presynaptic neuron contacts to postsynaptic neurons with the same neurotransmitter type (glutamatergic-glutamatergic neuron (glu-glu) (Fig. II.2b-1b) or GABA-GABA). In heterotypic-paired of neurons, the synaptic connections from a presynaptic neuron contacts postsynaptic neurons with different neurotransmitter types (glu-GABA).

In paired of neurons, we define the “output” responses of a neuron as synaptic responses generated from a presynaptic neuron. For example, the output postsynaptic current (PSC) amplitude from a neuron in a pair is the sum of autaptic and heterosynaptic PSC amplitudes generated from the same presynaptic neuron (Fig.

II.2b-1a and II.2b-2b). On the other hand, we define the “input response“ of a neuron in a pair as the synaptic response onto a postsynaptic neuron. For example, the input EPSC amplitude is the sum of autaptic PSC amplitude generated from itself and the heterosynaptic PSC amplitude generated from the partner neuron (Fig. II.2b-1 and II.2b-2). Importantly, in homotypic pairs, only input but not output RRP charges of a neuron can be measured by hypertonic solution application (Fig. II.2b-1). In the heterotypic pairs, the output RRP charges of a neuron can be measured separately by blocking glutamatergic or GABAergic responses pharmacologically (Fig. II.2b-2; Fig. IIIA.1A).

a

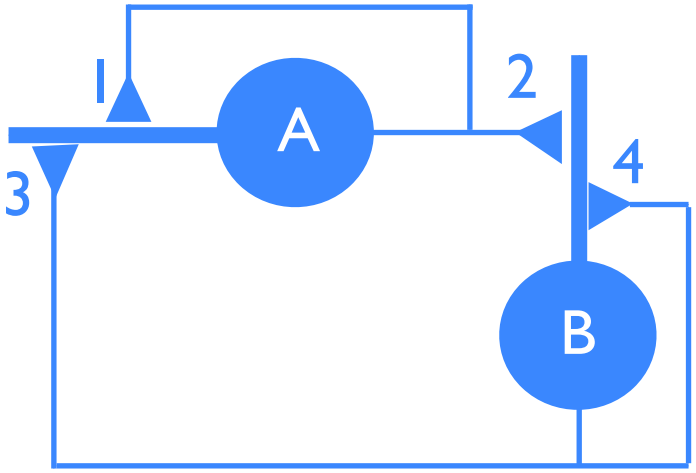

input of cell A = s1+s3
output of cell A = s1+s2
input of cell B = s2+s4
output of cell B = s3+s4

b

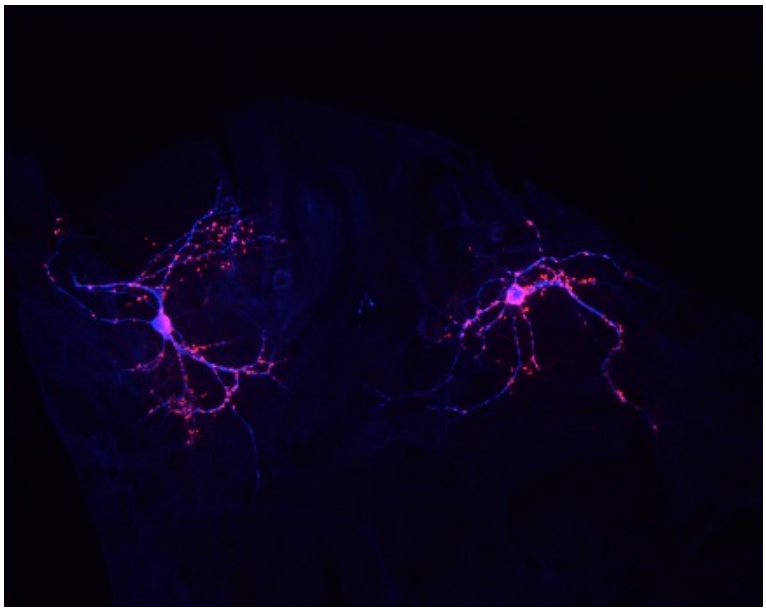

Figure II.2b-1 Diagrams illustrate the synaptic connections in a homotypic neuronal pair.

(a) Cartoon diagrams illustrate a homotypic neuronal pair: each neuron with same neurotransmitter type in a pair forms autaptic (synaptic connection 1 (s1) and s4) as well as heterosynaptic connections (s2 and s3). The synaptic input response of cell A is the sum of s1 and s3. Output response of cell A: sum of s1 and s2. Input response of cell B is the sum of s2 and s4. Output response of cell B: sum of s3 and s4. (b) Two glutamatergic neurons are grown on a glial island and labeled with VGLUT1 (red) and microtubule-associated protein 2 (MAP2) (blue) antibodies.

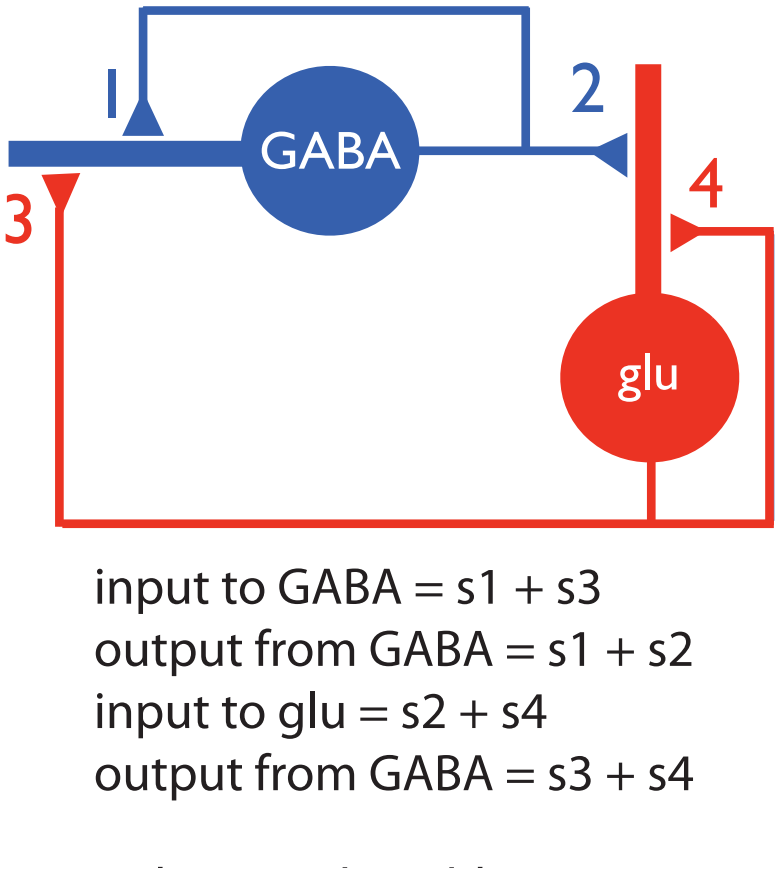

Figure II.2b-2 A diagram illustrates the synaptic connections in a heterotypic neuron pair

Heterotypic neuronal pair: each neuron with different neurotransmitter type in a pair (glu-GABA) forms autaptic (GABA: s1; glu: s4) as well as heterosynaptic (GABA: s2; glu: s3) connections. The synaptic input response of the GABAergic neuron is the sum of s1 and s3. Output response of the GABAergic neuron: sum of s1 and s2. Input response of the glutamatergic neuron: sum of s2 and s4. Output response of glutamatergic neuron: sum of s3 and s4.

I3. Methods to manipulate neuronal activity

To study how synapse formation and function can be modulated by activity, we manipulated neuronal activity by three ways. First, we applied tetrodotoxin (TTX) in the culture medium 6 days before recording. TTX blocks AP by binding to voltage gated sodium channels, which are responsible for triggering neurotransmitter release by responding to AP. Second, in order to study how glutamatergic synaptic activity affects synapse formation and function, we applied NBQX (2,3-dihydroxy-6-nitro-7-sulfamoyl-benzo [f]quinoxaline-2, 3-dione) and APV ((2*R*)-amino-5-phosphonovaleric acid; (2*R*)-amino-5-phosphonopentanoate) in the culture medium to block AMPA and NMDA receptors, respectively, during neuron development. Third, in order to study how the partner neuron's activity affects input/output of a neuron, we over-expressed Kir2.1 (potassium inward-rectify channel, subfamily J, member 2) channels specifically to either glutamatergic or GABAergic neurons. Kir2.1 channel is an inward rectify potassium channels, which has been used to suppress excitability in hippocampal neurons (Burrone et al., 2002; Hartman et al., 2006). Over expression of Kir2.1 hyperpolarizes the neuron and decreases its resting membrane resistance. Therefore, over expression of Kir2.1 causes the neuron to be less excitable than the control neurons.

I4. Application of two-neuron microculture:

To study the mechanisms involved in synapse formation regulated by MeCP2

A previous study showed that MeCP2 affects glutamatergic synaptic strength by regulating its synapse number (Chao et al., 2007) using male mice models either lacking MeCP2 ($MeCP2^{Null/y}$) (Chen et al., 2001; Guy et al., 2001) or overexpressing MeCP2 ($MeCP2^{Tg1/y}$) (Collins et al., 2004). In $MeCP2^{Null/y}$, the glutamatergic synapses number decrease compare to wild type neurons. In $MeCP2^{Tg1/y}$, the glutamatergic synapses increase compare to wild type neurons (Chao et al., 2007). However, the control mechanisms, such as whether the MeCP2 regulated factors responsible for synapse formation are located in the pre or the postsynaptic site, remain largely unknown

In this thesis, we further investigated whether the MeCP2 regulated factors are located at the pre- or the postsynaptic site that regulates synapse formation by separating pre- and postsynaptic mechanisms. We utilized a co-culture system that is composed of a paired of wild type (wt) and MeCP2 mutant neuron (either from $MeCP2^{Null/y}$ or $MeCP2^{Tg1}$ mice) on a glial island. We have tested two hypotheses to examine the possible cell autonomous mechanisms involved in MeCP2 regulated synapse formation: the postsynaptic model and the presynaptic model. The postsynaptic model proposes that if MeCP2-regulated molecules at the postsynaptic site are responsible for synapse formation, then removal of MeCP2 expression in a neuron will reduce synapse formation towards the same neuron, regardless of whether the synapses were made by itself or its wild type partner (Fig. II.4a-a). The presynaptic model proposes that if regulation of synapse number by MeCP2 is presynaptic, then autaptic and heterosynaptic synapses formed by the MeCP2-deficient neuron will be reduced (Fig. II.4a-b).

We first analyzed synaptic connections between a wild type and a MeCP2-mutant neuron by measuring the input and output synaptic strength. Since the synapse number is a determinant of RRP size and spontaneous release frequency (Chao et al., 2007). Therefore, we have used the size of input RRP (which is the sum of the RRP in autaptic connections and in heterotypic connections, to a neuron in a microcircuit) and frequency of input spontaneous release events (which is the sum of the spontaneous release frequency in autaptic connections and in heterotypic connections, to a neuron in a microcircuit) as indicators of synapse number made on a neuron. The possible outcomes of resulting synaptic parameters in the pre- or the post- synaptic model are listed in Table IH.1. Furthermore, we have also analyzed the synaptic efficiency such as PPR between each type of synaptic connection (wt to wt, wt to MeCP2, MeCP2 to wt, MeCP2 to MeCP2).

Clarifying whether the origin of the defect is pre- or postsynaptic using wt/MeCP2 mutant two-neuron culture is important in the identification of the possible downstream targets of MeCP2 that are critical for regulating glutamatergic synapse formation.

a

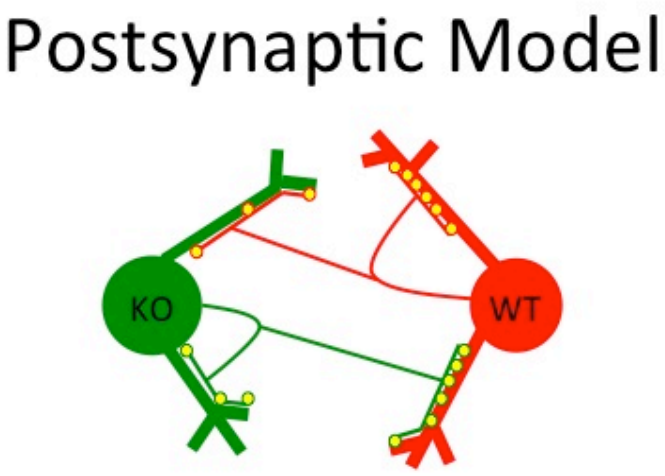

b

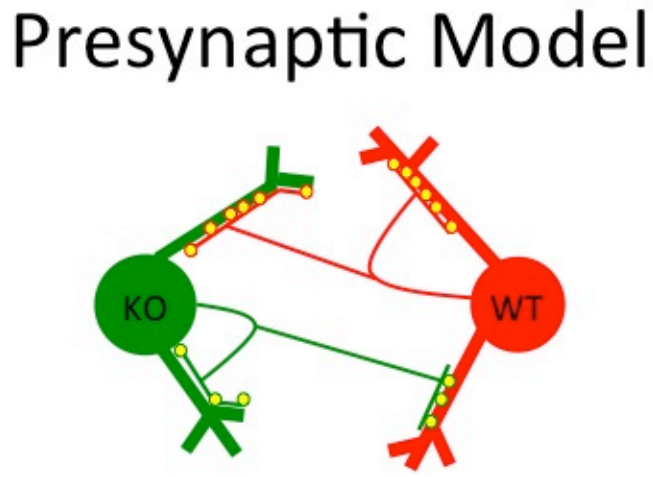

Figure II.4a Strategy to determine the location of the MeCP2 rate-limiting factor to the pre- or postsynaptic sites. A wild type (MeCP2-wild type (W), red) and a -mutant (e.g., MeCP2-knockout (KO); green) neuron were co cultured on a microisland. Synaptic responses were measured by paired-recording. (a) In postsynaptic model, the total synapses number made on the MeCP2-KO neuron will be less compared to the partner wild type neuron. (b) In presynaptic model, the total synapses number made from the MeCP2-KO neuron will be less compared to the partner wild type neuron.

a

Postsynaptic model	WT	MeCP2 KO
Input RRP size	Larger	Smaller
Input mEPSC frequency	Larger	Smaller
Output EPSC amplitude	Same	Same

b

Presynaptic model	WT	MeCP2-KO
Input RRP size	Same	Same
Input mEPSC frequency	Same	Same
Output EPSC amplitude	Larger	Smaller

Table II.1 The table illustrates the post- (a) and presynaptic (b) model, the expected relative input RRP size, input mEPSC and output EPSC amplitude between a wild type and a MeCP2-KO neuron in a circuit.

Chapter II
Materials and Methods

Part A

Neuronal Culture. Murine microisland cultures were prepared as described previously (Xue et al., 2007). Briefly, hippocampal neurons from newborn mice (P0-1) were plated at a density of 4000 neurons per 35 mm diameter dish. We then chose islands that contained a pair of neurons for recordings. Cells were used for electrophysiology and morphological analysis at days in vitro (DIV) 12-15. For experiments in which synaptic neuronal excitability was blocked, neurons were cultured in the presence of 0.5 µM TTX (Tocris Bioscience, Bristol, UK) added at DIV 6, 10 and 14. For experiments in which ionotropic glutamatergic receptors was blocked, neurons were cultured in the presence of 2 µM 2,3-dihydroxy-6-nitro-7-sulfamoyl-benzo[f]quinoxaline-2,3-dione (NBQX; Tocris Bioscience, Bristol, UK) and 100 µM D-(-)-2-Amino-5-phosphonopentanoic acid (APV; Tocris Bioscience, Bristol, UK) or 10µM Philanthotoxin-433 (Sigma-Aldrich, St. Louis, MO, USA) added at DIV 6, 10 and 14.

To facilitate the visual detection of GABAergic neurons, in most experiments we cultured neurons from GAD67-GFP (Δneo)/+ (GAD67) mice, in which GABAergic neurons are fluorescently labeled (Tamamaki et al., 2003). Comparison of electrophysiological response properties of striatal GAD67-GFP (Δneo)/+ and wild type neurons revealed no significant differences in synaptic properties (spontaneous miniature IPSCs (mIPSCs) amplitudes: WT single neuron; 43.6±2.6 pA, WT paired; 37.7±3.5 pA; GAD67 single; 38.8±2.6 pA, GAD67 paired; 42.2±2.3 pA, $p>0.05$; vesicular release probabilities (P_{vr}): WT single; 14.0±2.3 %, WT paired; 12.3±2.6 %; GAD67 single; 14.3±2.3 %, GAD67 paired; 13.9±1.7% $p>0.05$). To express Kir2.1 specifically in either glutamatergic or GABAergic neurons, we cultured hippocampal neurons from Viaat-cre mice and then infected them with lentiviral constructs (see below).

Lentivirus constructs and production. For expression of Kir2.1, we made use of the Cre/LoxP recombination system in combination with two lentiviral shuttle vectors and Viaat promoter driven expression of Cre recombinase ((Chao et al., 2010), Viaat Cre mice). For glutamatergic expression, we used a floxed lentiviral shuttle vector in which a synapsin promoter controlled expression cassette of Kir2.1 fused to nuclear

localization sequence-tagged green fluorescent protein (NLS-GFP) via a self-cleaving P2A peptide (Kim et al., 2011) (Kim et al., 2011) is framed by two likewise-oriented mutant LoxP sites (LE/RE mutation) (f(syn)FLOX(NLS-GFP-P2A-Kir2.1)). In GABAergic cells, Viaat promoter driven Cre expression causes the deletion of the NLS-P2A-Kir2.1 transgene, resulting in no NLS-GFP or Kir2.1 expression (Albert et al., 1995; Araki et al., 1997). For expression of Kir2.1 in GABAergic neurons, we used a synapsin promoter controlled Cre-recombinase-dependent lentiviral expression system carrying a reversed and double-floxed NLS-GFP-P2A-Kir2.1 transgene with two nested pairs of incompatible mutant (LE/RE) lox sites (LoxP and Lox2722). A red fluorescent protein (RFP) transgene was cloned in sense orientation between the first two lox sites (f(syn)LoxP_RFP_Lox2722_reverseNLS-GFP-P2A-Kir2.1_LoxP_Lox2722). In this configuration, RFP is only expressed in non-Cre expressing cells. In Viaat-Cre GABAergic neurons, Cre expression leads to a switch from RFP to NLS-GFP and Kir2.1 translation due to excision and inversion events by Cre at the lox sites (Sohal et al., 2009). The resulting two lox sites are incompatible and double mutant to prevent further genomic recombination (Albert et al., 1995; Araki et al., 1997; Sohal et al., 2009). Control pairs for each of the cell type specific Kir2.1 expression groups were infected with constructs as described above lacking the sequence for Kir2.1.

The preparation of lentiviral particles expressing these transgenes was done as described (Lois et al., 2002). Briefly, HEK293T cells were cotransfected with 10µg shuttle vector and the helper plasmids pCMVdR8.9 and pVSV.G (5µg each) with X-tremeGENE 9 DNA transfection reagent (Roche Diagnostic, Germany). After 72h the virus containing cell culture supernatant was collected and purified by filtration. Aliquots were flash-frozen in liquid nitrogen and stored at -80°C. Estimation of the titer was done on mass cultures of wild-type hippocampal neurons. For infection, 150 µl of virus ($6x10^5$-$1x10^6$ IU/ml) harboring either shuttle vector was pipetted onto 1 DIV hippocampal Viaat-Cre neurons.

Electrophysiology. Whole-cell voltage-clamp recordings were performed with a patch-clamp amplifier (MultiClamp 700B amplifier; Molecular Devices, Sunnyvale, CA) under the control of Clampex 9.2 (Molecular Devices). Data were acquired at 10 kHz and low-pass filtered at 3 kHz. The holding potential was –70 mV. The series

resistance was compensated at 70 % and only cells with series resistances below 10 MΩ were analyzed. The pipette resistance was between 2-5 MΩ. The standard extracellular solution contained (in mM): NaCl, 140; KCl, 2.4; HEPES, 10; glucose, 10; $CaCl_2$, 2; and $MgCl_2$, 4 (all listed reagents from Carl Roth, Karlsruhe, Germany; 300 mOsm; pH 7.4). Hypertonic solution for measuring RRP size was made by adding 500 mM sucrose (Sigma-Aldrich, St. Louis, MO, USA) to the standard extracellular solution. The patch pipette solution contained (in mM): KCl, 136; HEPES, 17.8; EGTA (Carl Roth), 1; $MgCl_2$, 0.6; ATP-Mg (Sigma-Aldrich), 4; GTP-Na (Sigma-Aldrich), 0.3; Phosphocreatine (Calbiochem, MERCK, Darmstadt, Germany), 12; and Phosphocreatine kinase (Sigma-Aldrich), 50U ml^{-1} (300 mOsm; pH 7.4). This solution set the reversal potential of IPSCs and EPSCs to approximately 0 mV and produced readily quantifiable inward currents in both excitatory and inhibitory neurons.

Step depolarization (to 0 mV, 2 ms) was applied sequentially (with 2 s delay) to each neuron to induce unclamped action potentials in the axon, resulting in pairs of autaptic and heterosynaptic postsynaptic currents (PSCs). The size of the readily releasable pool (RRP) was determined by 4 or 5 s application of a pool-depleting hypertonic sucrose solution. The RRP was quantified by first base lining the steady-state current at the end of the hypertonic response and then integrating the charge of the transient synaptic current component.

In heterotypic pairs (glu-GABA), quantification of PSC, RRP and P_{vr} was accomplished by consecutively blocking the glutamatergic and GABAergic PSC components with kynurenic acid (3 mM; Tocris Bioscience) and bicuculline (30 µM; Tocris Bioscience), respectively. We compared the amplitudes of output PSCs (Figure 1A; sum of autaptic and heterosynaptic PSCs) and the sizes of output RRPs (Figure 1A; sum of the autaptic and heterosynaptic hypertonic sucrose-evoked responses) from heterotypic glu-GABA neuronal pairs to the amplitudes of output PSCs and the sizes of input RRPs from homotypic (glu-glu or GABA-GABA) pairs. The input RRP in a homotypic pair is the sum of autaptic and heterosynaptic connections onto a neuron, as the contribution of each neuron is not pharmacologically distinguishable in this configuration. However, the amplitudes of output PSC and sizes of input RRP were comparable between the two neurons in glu-glu (output PSC: $p = 0.78$; input RRP: $p =$

0.72) or GABA-GABA pairs (output PSC: $p = 0.20$; input RRP: $p = 0.21$). Therefore, we assumed that the sizes of output RRP were comparable to the sizes of input RRP in glu-glu and GABA-GABA pairs. To calculate vesicular release probability (P_{vr}), the charge of evoked response was integrated (1 s for EPSC; 2 s for IPSC) and divided by the RRP charge. In glu-glu and GABA-GABA pairs, the mean vesicular release probability of autaptic and heterosynaptic connections ending at a common postsynaptic neuron (input P_{vr}), was calculated by dividing the sum of a neuron's input autaptic PSC charge and input heterosynaptic PSC charge from the partner neuron by its input RRP charge. Therefore, input P_{vr} does not distinguish properties of autaptic and heterosynaptic connections. As an alternative measure of the synaptic release efficiency, a pair of PSCs was stimulated at a specific interval (EPSCs 25 ms; IPSCs 100 ms) and the paired-pulse ratio (PPR) was computed by dividing the second PSC amplitude by the first (PPR = EPSC2/EPSC1 and IPSC2/IPSC1). Spontaneous release was detected as described previously (Clements and Bekkers, 1997).

For recording the current-voltage relationship of EPSCs, the presynaptic neuron (glutamatergic) was stimulated by step depolarization with KCl pipette solution (see above). Whole-cell currents were obtained in the postsynaptic neurons (glutamatergic or GABAergic) with the pipette solution contained (mM): CsCl, 143; HEPES, 20; EGTA (Carl Roth), 1; $MgCl_2$, 0.6; ATP-Mg (Sigma-Aldrich), 4; GTP-Na (Sigma-Aldrich), 0.3; Phosphocreatine (Calbiochem, MERCK, Darmstadt, Germany), 12; and Phosphocreatine kinase (Sigma-Aldrich), 50U ml^{-1}; QX314, 2; spermine, 0.05 (300 mOsm; pH 7.4). APV (100uM) and bicuculline (30uM) were present in the extracellular solution to isolate (AMPA receptor) responses. Current-voltage plots were generated by plotting the EPSC amplitudes at holding potentials of -80 to +40 mV with 20 mV increments. The current-voltage relationship in control and Kir2.1 expressing neurons in a glu-GABA pair were obtained by recording the current response to hyperpolarizing steps from -80 to -110 with 10 mV decrements with KCl pipette solution (see above).

Data were analyzed offline using AxoGraph X (Axo-Graph Scientific, Sydney, Australia), KaleidaGraph (Synergy Software, Reading, PA, USA) and Prism5 (GraphPad, San Diego, CA, USA). Statistical significance was tested using the Student's t-test for two groups with normal distribution and one-way ANOVA with a Tukey post hoc test for three or more groups.

Immunocytochemistry and morphological analysis. Quantification of dendritic tree size and synapse type and number was performed using combined immunocytochemical staining for MAP2, VGLUT1 and VGAT. Microisland cultures from C57/Black6 mice were fixed at DIV 12-15 with 4 % paraformaldehyde (Sigma-Aldrich) and permeabilized with 0.02 % Tween-20 in phosphate-buffered saline (PBST). After blocking with 4 % normal goat serum (NGS; Jackson ImmunoResearch, Suffolk, UK) in PBST for 1 h at room temperature, the specimens were incubated overnight at 4 °C with guinea pig anti-VGLUT1 (1:4000, Synaptic Systems, Gottingen, Germany), mouse anti-VGAT (1:1000, Synaptic Systems) and chicken anti-MAP2 (1:2000; Chemicon, Millipore, Billerica, MA, USA). After washing 3 times with PBST for 10 minutes, cells were incubated for 1.5 h at room temperature in 4 % NGS containing the appropriate secondary antibody (Alexa-488, -555, -647, 1:1000; Molecular probes, Invitrogen, Eugene, OR, USA). The specimens were then washed three times with PBS for 15 minutes and mounted on glass slides with Prolong Gold Antifade Reagent (Molecular probes, Invitrogen, Eugene, OR, USA). The fluorescence signals were visualized on an Olympus IX 81 microscope with a 20x, 0.75 NA objective lens and images were captured with a CCD camera (Princeton MicroMax, Roper Scientific).

Image analysis was performed using ImageJ. The type of neuron (GABAergic/glutamatergic) was identified by elevated fluorescence signals for VGLUT1 or VGAT at the cell soma (Hartman et al., 2006). The associated dendrites were determined by tracing using MAP2 staining. The density of synapses along three randomly chosen dendrites was determined by manual counting. Total dendritic length was quantified by measuring the length of all MAP2-positive processes using a custom-written plug-in in Image J (Neuron J; NIH). Total number of glutamatergic and GABAergic synapses were quantified by fluorescence signals for VGLUT1 and VGAT, respectively, using custom Macro in ImageJ. All data processing was performed using Microsoft (Seattle, WA, USA) Excel, KaleidaGraph (Synergy Software, Reading, PA, USA) and Prism5 (GraphPad, San Diego, CA, USA). Statistical significance was tested using Student's t-test for two groups with normal distribution and one-way ANOVA with a Tukey post hoc test for three or more groups.

Part B

Neuronal Culture. Murine microisland culturing was performed as described previously. For autaptic neuron and paired of neuron experiment, neurons from newborn mice (P0-1) were plated at a density of 4000 neurons for hippocampal neurons per 35mm diameter dish. We then chose islands that contained either a single neuron or a pair of neurons for the recordings. Cells were used for electrophysiology and morphological analysis at days in vitro (DIV) 12-15.

MeCP2 mutant neuronal culture. MeCP2$^{Null/Y}$ male mice are on a C_{57}BLJ6 background, *MeCP2*^{Tg1} male mice are on a FVB background. Mutant mice and control mice were obtained from the same litter. For mixed culture experiment, after trituration, the wild type and MeCP2-mutant cell suspension were incubated in PKH26 and PKH67, respectively (describe below) or infected with viruses (describe below). After labeling or infection, the wild type and MeCP2-mutant cells were mixed at equal number and plated on to micro island culture at the density of 4000 neurons per 35mm diameter dish. We then only chose islands that contained one wild type and one MeCP2 mutant neuron for experiments.

Lentivirus Constructs, Production and Infection. To visualize synapses from each neuron of a pair of neurons on a micro island two lentiviruses were deployed. Their shuttlevectors bearing a synapsin promoter controlled expression cassette of either a nuclear localized GFP or RFP coupled via a self-cleaving P2A peptide (Kim et al., 2011) to synaptophysin that is C-terminally tagged by m-Kate2 or GFP (NLS-GFP-P2A-Sypmkate2, NLS-RFP-P2A-SypGFP). The preparation of lentiviral particles expressing these transgenes was done as described (Lois et al., 2002). Briefly, HEK293T cells were cotransfected with 10µg shuttle vector (F(syn)nGFP-P2A-Sypmkate2-w and F(syn)nRFP-P2A-SypGFP-w) and the helper plasmids pCMVdR8.9 and pVSV.G (5µg each) with X-tremeGENE 9 DNA transfection reagent (Roche Diagnostic, Germany). After 72h the virus containing cell culture supernatant was collected, purified by filtration and concentrated via centrifugation through a Amicon Ultra centrifugal filter (Merck-Millipore, Germany). Aliquots of the concentrate were flash-frozen in liquid nitrogen and stored at -80°C. Estimation of the titer was done on mass cultures of wild-type hippocampal neurons. For infection 100 µl of concentrated

virus (1.5-1.6x10^7 IU/ml) expressing either the m-Kate2 or GFP tagged Synaptophysin were incubated with freshly prepared 2x10^5 wild type or MeCP2 mutant neurons in a 1.5 ml microcentrifuge tube at 37°C for 3 hours. Subsequently cells were purified from residual viral supernatant by centrifugation (150 x *g*), washed two times and resuspended in culture medium before plating onto astrocytes.

PKH26/67 staining. Culture neurons were stained with PKH26 or PKH67 according to the manufacturer's protocol (Sigma-Aldrich, St. Louis, MO, USA). 5x10^5 neurons were resuspended in Diluent C and the dye were diluted in Diluent C to the concentration of 8x10^{-6}M. The PKH26 and PKH67 were added to the cell suspension for 5 min at room temperature. Next, dye reaction were stop by adding 10% serum. Excess dye was removed by centrifuging the cell suspension (150 x *g*), washed twice. The cell pellet were resuspeneded in culture medium.

Electrophysiology. Whole-cell voltage-clamp recordings were performed with a patch clamp amplifier (MultiClamp 700B amplifier; Molecular Devices, Sunnyvale, CA) under the control of Clampex 9.2 (Molecular Devices). Data were acquired at 10 kHz and low-pass filtered at 3 kHz. The holding potential was –70 mV. The series resistance was compensated at 70 % and only cells with series resistances below 10 MΩ were analyzed. The pipette resistance was between 2-4 MΩ. The standard extracellular solution contained (in mM) NaCl, 140; KCl, 2.4; HEPES, 10; glucose, 10; $CaCl_2$, 2; and $MgCl_2$, 4 (all listed reagents from Carl Roth, Karlsruhe, Germany; 300 mOsm; pH 7.4). Hypertonic solution for measuring RRP size was made by adding 500 mM sucrose (Sigma-Aldrich, St. Louis, MO, USA) to the standard extracellular solution. The patch pipette solution contained (in mM) KCl, 136; HEPES, 17.8; EGTA (Carl Roth), 1; $MgCl_2$, 0.6; ATP-Mg (Sigma-Aldrich), 4; GTP-Na (Sigma-Aldrich), 0.3; Phosphocreatine (Calbiochem, MERCK, Darmstadt, Germany), 12; and Phosphocreatine kinase (Sigma-Aldrich), 50U ml^{-1} (300 mOsm; pH 7.4).

Step depolarizations (to 0 mV, 2 ms) were applied sequentially (with 2 s delay) to each neuron to induce unclamped action potentials in the axon, resulting in pairs of autaptic and heterosynaptic excitatory postsynaptic currents (EPSCs). The size of the readily releasable pool (RRP) was determined by 4 s application of a pool-depleting hypertonic sucrose solution. The size of RRP was quantified by first base lining the

steady state current at the end of the hypertonic response and then integrating the charge of the transient synaptic current component. To calculate vesicular release probability (P_{vr}), the charge of evoked response was integrated (1 s) and divided by the RRP charge. Input P_{vr}, the mean vesicular release probability of autaptic and heterosynaptic connections ending at a common postsynaptic neuron, was calculated by adding the autaptic and heterosynaptic EPSC charge to the input RRP charge. Input P_{vr} is therefore not able to distinguish between the properties of autaptic and heterosynaptic connections. As an alternative measure of the synaptic release efficiency, a pair of EPSCs was stimulated at a specific interval (25 ms) and the paired-pulse ratio (PPR) was computed by dividing the second EPSC amplitude by the first (PPR = EPSC2/EPSC1). Spontaneous release was detected as described previously.

Data were analyzed offline using AxoGraph X (Axo-Graph Scientific, Sydney, Australia), KaleidaGraph (Synergy Software, Reading, PA, USA) and Prism5 (GraphPad, San Diego, CA, USA). Statistical significance was tested as indicated in the figure texts using the Student's t-test for two groups with normal distribution, One-way ANOVA with a Tukey post hoc test for three or more groups, and Pearson correlation to quantify the association between two groups.

Morphology. Quantification of synapse number was performed using immunocytochemical staining for MAP2. Neurons were fixed at DIV 12-15 with 4 % paraformaldehyde (Sigma-Aldrich) and permeabilized with 0.02 % Tween-20 in phosphate-buffered saline (PBST). After blocking with 4 % normal goat serum (NGS; Jackson ImmunoResearch, Suffolk, UK) in PBST for 1 h at room temperature, the specimens were incubated overnight at 4 °C with chicken anti-MAP2 (1:2000; Chemicon, Millipore, Billerica, MA, USA). After washing 3 times with PBST for 10 minutes, cells were incubated for 1.5 h at room temperature in 4 % NGS containing the appropriate secondary antibody (Alexa-647, 1:2000; Molecular probes, Invitrogen, Eugene, OR, USA). The specimens were then washed three times with PBS for 15 minutes and mounted on glass slides with Prolong Gold Antifade Reagent (Molecular probes, Invitrogen, Eugene, OR, USA). The fluorescence signals were visualized on an Olympus IX 81 microscope with a 20x, 0.75 NA objective lens and images were captured with a CCD camera (Princeton MicroMax, Roper Scientific). Image analysis

was performed using ImageJ. The density of synapses along dendrites was determined by manual counting. All data processing was performed using Microsoft (Seattle, WA, USA) Excel, KaleidaGraph (Synergy Software, Reading, PA, USA) and Prism5 (GraphPad, San Diego, CA, USA). Statistical significance was tested using Student's t-test for two groups with normal distribution and one-way ANOVA with a Tukey post hoc test for three or more groups.

Chapter III
Results

Part A

Basic synapse properties in mixed glutamatergic-GABAergic pairs

To explore the effects of neurotransmitter identity interplay on synaptic characteristics, we examined pairs of hippocampal neurons grown on a glial microisland (see Materials and Methods), where one cell was glutamatergic and the other GABAergic. As shown in Figure 1A, four types of synaptic connections can be found in a glutamatergic-GABAergic (glu-GABA) pair. To characterize the synaptic properties at each of the four types of connections, we pharmacologically separated the postsynaptic current (PSC) and readily releasable pool (RRP) responses for glutamatergic and GABAergic connections by consecutively applying the $GABA_A$ receptor antagonist bicuculline and the glutamatergic receptor antagonist kynurenic acid (30 μM and 3mM, respectively; Fig. IIIA.1B).

To examine whether the postsynaptic neuron's neurotransmitter phenotype influences synaptic parameters of the presynaptic neuron, we compared the amplitudes of output PSCs (sum of autaptic and heterosynaptic PSCs) and the sizes of output RRPs (sum of the autaptic and heterosynaptic hypertonic sucrose-evoked responses) from heterotypic glu-GABA neuronal pairs to the amplitudes of output PSCs and the sizes of input RRPs from homotypic (glu-glu or GABA-GABA) pairs. The input RRP in a homotypic pair is the sum of autaptic and heterosynaptic connections onto a neuron, as the contribution of each neuron is not pharmacologically distinguishable in this configuration. However, the amplitudes of output PSC and sizes of input RRP were comparable between the two neurons in glu-glu (output PSC: p = 0.78; input RRP: p = 0.72) or GABA-GABA pairs (output PSC: p = 0.20; input RRP: p = 0.21). Therefore, we assumed that the sizes of output RRP were comparable to the sizes of input RRP in glu-glu and GABA-GABA pairs. We found that in glutamatergic neurons, the output excitatory postsynaptic currents (EPSCs) and output RRPs were similar with either a glutamatergic or GABAergic partner neuron (Fig. IIIA.1C). Conversely, while the GABAergic neurons displayed similar output inhibitory postsynaptic current (IPSC) responses in glu-GABA and GABA-GABA cell pairs, the output RRP sizes increased 2.5±0.3 fold with glutamatergic input (glu-GABA pair) compared to GABAergic input (GABA-GABA pair; Fig. IIIA.1C).

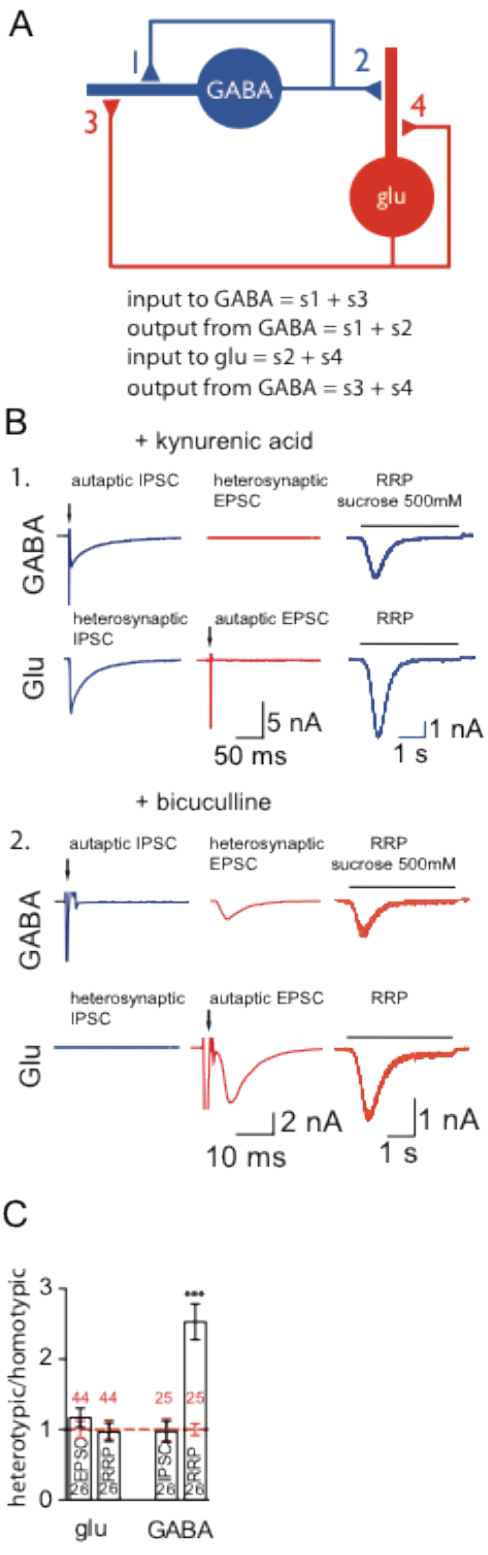
A
GABA
glu
1
2
3
4
input to GABA = s1 + s3
output from GABA = s1 + s2
input to glu = s2 + s4
output from GABA = s3 + s4
B
+ kynurenic acid
1.
autaptic IPSC
heterosynaptic EPSC
RRP sucrose 500mM
GABA
heterosynaptic IPSC
autaptic EPSC
RRP
Glu
5 nA
50 ms
1 nA
1 s
+ bicuculline
2.
autaptic IPSC
heterosynaptic EPSC
RRP sucrose 500mM
GABA
heterosynaptic IPSC
autaptic EPSC
RRP
Glu
2 nA
10 ms
1 nA
1 s
C
heterotypic/homotypic
3
2
1
0
44
44
25
25
***
EPSC
RRP
IPSC
RRP
26
26
26
26
glu
GABA

Figure IIIA.1 GABAergic output is modulated by glutamatergic input in glu-GABA pair.

(A) A schematic diagram illustrating four different synaptic connections in a glu-GABA neuronal circuit. The axon from a glutamatergic or a GABAergic neuron makes synapses onto itself and the partner neuron. 1: GABA autapse; 2:GABA heterosynapse; 3: glu heterosynapse; 4: glu autapse. (B) Representative traces of evoked PSCs and sucrose responses from paired recording of a GABAergic (upper traces) and glutamatergic (lower traces) neuron pair. Responses from autaptic and heterosynaptic connections of each cell and were recorded in the presence of kynurenic acid (B1) or bicuculline (B2). Arrow indicates 2 ms somatic depolarization. The number under each trace represents the synaptic connections shown in (A). (C) Bar graph showing the mean output PSC (EPSC, IPSC) amplitudes and output RRP charges measured in heterotypic neuronal pairs normalized to those recorded in homotypic pairs from the same culture (red dashed line). All values are mean ± SEM. $^{***}p \leq 0.001$. Numbers in bar graphs are n values.

Glutamatergic input modulates the efficiency of GABAergic synapses

An increase in the GABAergic RRP size with no change in synaptic output IPSCs with glutamatergic innervation suggests a change in synaptic efficiency. To study synaptic efficiency, we measured the vesicle release probability (P_{vr}) and paired-pulse ratio (PPR) of glutamatergic and GABAergic neurons in glu-GABA pairs, glu-glu, and GABA-GABA pairs. Indeed, we found that the GABAergic synapses in glu-GABA pairs displayed significantly lower P_{vr} and higher PPR compared to GABA-GABA pairs (Fig. IIIA.2A, IIIA.2B; P_{vr}: GABA-GABA 20.6 ± 1.6 %; glu-GABA 9.7 ± 0.6 %; $p < 0.0001$; PPR: GABA-GABA 0.49 ± 0.02; glu-GABA 0.72 ± 0.02; $p < 0.0001$). Conversely, in glutamatergic neurons, the output P_{vr} and PPR values were comparable in either glu-glu or glu-GABA pairs (Fig. IIIA.2A, IIIA.2B; P_{vr}: glu-glu 5.9 ± 0.5 %; glu-GABA 6.8 ± 0.5 %; $p = 0.24$; PPR: glu-glu 1.32 ± 0.04; glu-GABA 1.27 ± 0.03; $p = 0.23$). This suggests that while glutamatergic innervations to a GABAergic neuron may increase the total vesicles available for release, it decreases the release probability for each vesicle.

To examine if the decrease in GABAergic synaptic efficiency in the glu-GABA pair is target cell specific, we compared the P_{vr} and PPR from the four connections in glu-GABA pairs to those in glu-glu and GABA-GABA pairs. While the overall efficiency of GABAergic output P_{vr} and PPR decreased upon glutamatergic innervations, the P_{vr} and PPR of GABAergic autapses and heterosynapses were comparable within each pair configuration (Fig. IIIA.2C). Glutamatergic autapses and heterosynapses showed similar P_{vr} and PPR values both within and between glu-GABA and glu-glu pairs (Fig. IIIA.2C). These data suggest that the decrease in synaptic release efficiency that occurs in GABAergic synapses in response to glutamatergic input happens in a cell-wide manner and is not target cell specific.

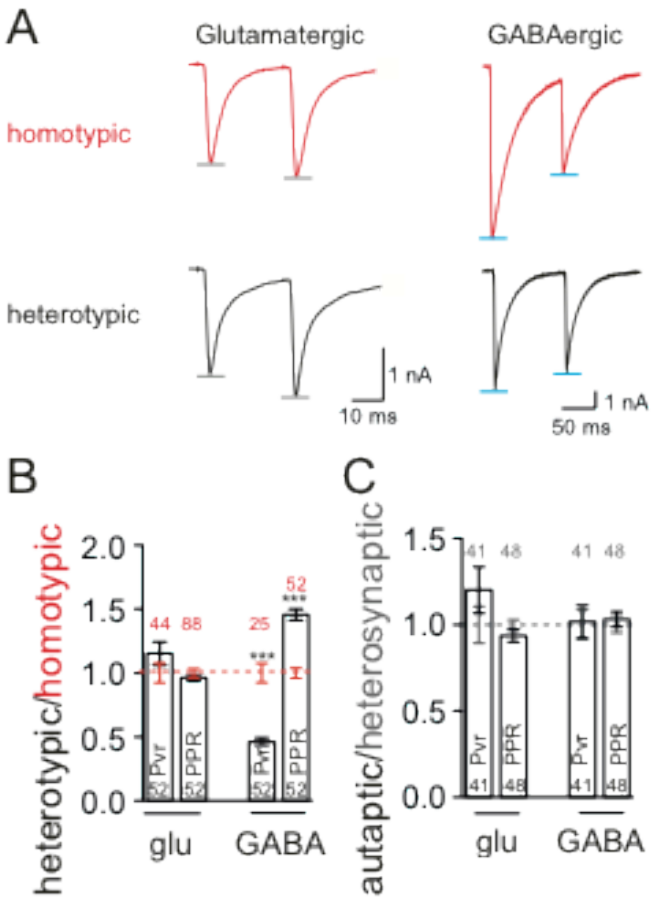
A
Glutamatergic
GABAergic
homotypic
heterotypic
1 nA
10 ms
1 nA
50 ms
B
heterotypic/homotypic
2.0
1.5
1.0
0.5
0.0
44
88
25
52
***
***
Pvr
PPR
52
52
52
52
glu
GABA
C
autaptic/heterosynaptic
1.5
1.0
0.5
0.0
41
48
41
48
Pvr
PPR
41
48
41
48
glu
GABA

Figure IIIA.2 Glutamatergic input affects GABAergic synaptic efficiency in glu-GABA pair. (A) Representative traces of paired-pulse EPSC (left) and IPSC (right) traces from heterosynaptic connections in homotypic (glu-glu, GABA-GABA; red traces) and heterotypic (glu-GABA; black traces) pairs. (B) Bar graph showing the P_{vr} and PPR in either glutamatergic or GABAergic neurons in glu-GABA pairs normalized to the mean value from homotypic pairs from the same culture (red dashed line). $^{***}p \leq 0.001$. (C) Bar graph showing the autaptic PPR and P_{vr} in glu-GABA neuronal pairs normalized to the heterosynaptic PPR and P_{vr} in glu-GABA neuronal pairs from the same pair (grey dashed line). All values are mean ± SEM. Numbers in bar graphs are n values.

Increased GABAergic synapse number contributes to increased RRP size

The larger output RRP sizes of GABAergic neurons with glutamatergic innervation may suggest proliferation of GABAergic synapses. To test this, we compared the total synapse numbers using immunocytochemical methods (Fig. IIIA.3A). We measured total synapse glutamatergic and GABAergic number using VGLUT1 and VGAT staining, respectively. In isolated glutamatergic neurons, the glutamatergic synapse number was comparable to the number of glutamatergic synapses in glu-GABA pairs and the synapse number per cell in glu-glu pairs (total number of VGLUT1 positive synapses divided by two; Fig. IIIA.3B). In contrast, the number of GABAergic synapses in glu-GABA pairs was significantly larger than the synapse number of single GABAergic neurons and the synapse number per cell in GABA-GABA pairs (total number of VGAT positive synapses divided by two; Fig. IIIA.3C). This suggests that in the two-neuron microcircuit a glutamatergic neuron makes the same total number of synaptic contacts independent to the postsynaptic neuron. However, the GABAergic neuron in a two-neuron microcircuit makes a higher number of total synaptic contacts with glutamatergic input.

A

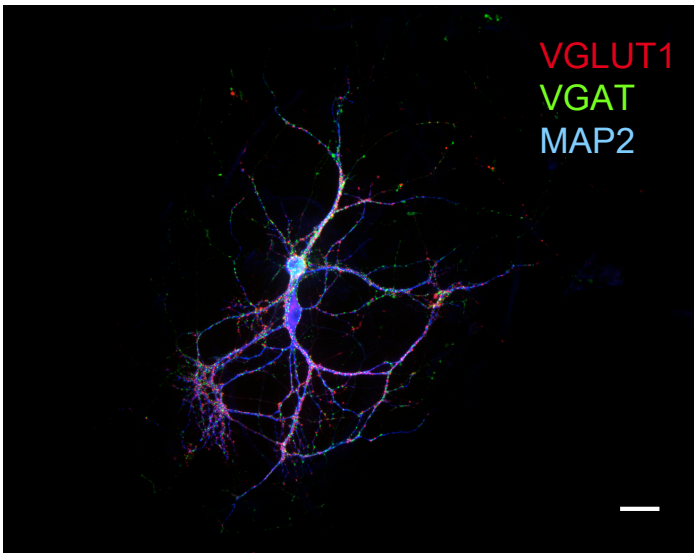
VGLUT1
VGAT
MAP2

B

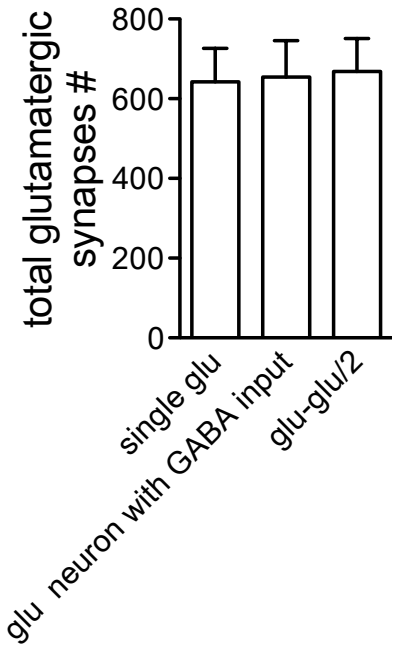
total glutamatergic synapses #
800
600
400
200
0
single glu
glu neuron with GABA input
glu-glu/2

C

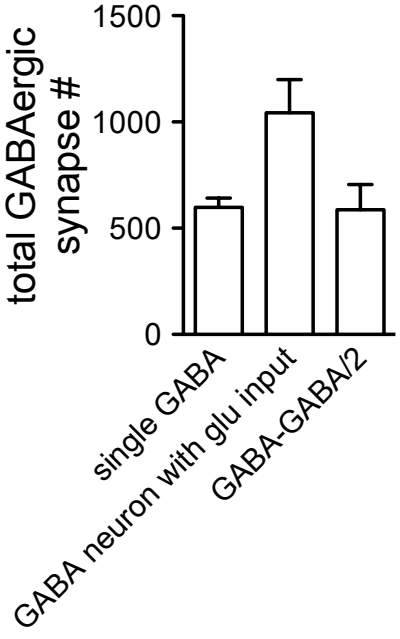
total GABAergic synapse #
1500
1000
500
0
single GABA
GABA neuron with glu input
GABA-GABA/2

Figure IIIA.3 Glutamatergic input causes increase in number and density of GABAergic synapses. (A) Representative images showing co-localization of VGLUT1 (red) and VGAT (green) with MAP2 (blue) immunofluorescence signals in a glu-GABA neuronal pair. Scale bar = 25 μm. (B) Bar graph showing the total number of VGLUT1 puncta makes from a glutamatergic neuron alone, glu-GABA neuronal pairs and glu-glu neurons. Noted that VGLUT1 puncta number per neuron is shown for glu-glu pairs. (C) Same as (B) for the number of VGAT puncta makes from GABAergic neurons. $^{**}p \leq 0.01$; $^{***}p \leq 0.001$.

Neuronal activity is required for the modulation of GABAergic synapse formation and function in glu-GABA pairs

How do the inputs from glutamatergic neurons modulate the synapses of GABAergic neurons? One possible mechanism may involve increased neuronal activity, as this has been found to modulate glutamatergic and GABAergic synapse formation and function in mass culture preparations (Burrone et al., 2002; Hartman et al., 2006). To test this, we blocked neuronal activity with tetrodotoxin (TTX, 0.5 μM) treatment of our cultures at 6-7 days in vitro (DIV), 6 days before recording. We found that TTX treatment blocked the effect of glutamatergic innervations on GABA synapse formation and function, as the GABAergic RRP size in TTX-treated glu-GABA pairs was similar to that in GABA-GABA pairs with and without TTX treatment (Fig. IIIA.4A). Furthermore, the GABAergic synapse density was significantly decreased compared to that in untreated pairs (Fig. IIIA.4B). Total number of synapses for a given presynaptic neuron was significantly decreased in GABAergic neurons but not in glutamatergic neurons (glutamatergic, non-treated: 536 ± 98 and TTX: 489 ± 92; p = 0.74; GABAergic, non-treated: 1027 ± 177 and TTX: 425 ± 68, p =0.0089). Our findings are consistent with previous work showing that suppression of network activity leads to a decreased density of GABAergic synapses in mass cultures (Hartman et al., 2006). Furthermore, we tested the effect of TTX treatment on the output of each neuron in the glu-GABA pair. P_{vr} and PPR of GABAergic neurons in TTX-treated glu-GABA pairs were also reversed compared to the level of GABA-GABA pairs with and without TTX treatment (Fig. IIIA.4C-D). TTX treatment did not affect the P_{vr} of glutamatergic neurons in either glu-GABA or glu-glu pair configurations (non-treated, P_{vr}: glu-GABA: 6.2 ± 0.6 %; glu-glu: 5.9 ± 0.5 %; p = 0.07; TTX: P_{vr}, glu-GABA: 5.3 ± 0.6%; glu-glu: 5.0 ± 0.7 %; p = 0.3).

Next we decreased neuronal activity by blocking ionotropic glutamate receptors using NBQX (10μM) and APV (50μM) treatment during synapse development (6-7 DIV, 6 days before recording). Again we found that GABAergic neurons in antagonist-treated glu-GABA pairs had decreased output RRP, PPR and increased P_{vr} with respect to untreated pairs (Fig, IIIA.4A, IIIA.4C-D, respectively), but we saw no change in the glutamatergic synapse properties (non-treated, output RRP: 0.97 ± 0.1 nC;

NBQX/APV (N/A), output RRP: 1.23 ± 0.1 nC; p = 0.28; non-treated, P_{vr}: 6.2 ± 0.6 %; N/A, P_{vr}: 5.15 ± 0.9 %; p= 0.23; non-treated, PPR: 1.30 ± 0.1; N/A, PPR: 1.32 ± 0.1; p = 0.90). Thus, chronic activity blockade reversed the synaptic output of GABAergic neurons that we observed in glu-GABA pairs to the level of GABA-GABA pairs. Specific inhibition of GluA2-lacking AMPA receptors with philanthotoxin-433 treatment during development (10 µM, 6 days before recording) also impaired the GABAergic output modification by decreasing RRP sizes and increasing synaptic efficiency (data not shown; see Discussion). This indicates that GABAergic synaptic output modification in glu-GABA pairs requires neuronal activity and ionotropic glutamatergic receptor activation. Furthermore, the lack of effect in glutamatergic neurons suggests that glutamatergic synapse formation does not require neuronal activity as suggested by previous studies (Craig et al., 1994; Rao and Craig, 1997; Gomperts et al., 2000).

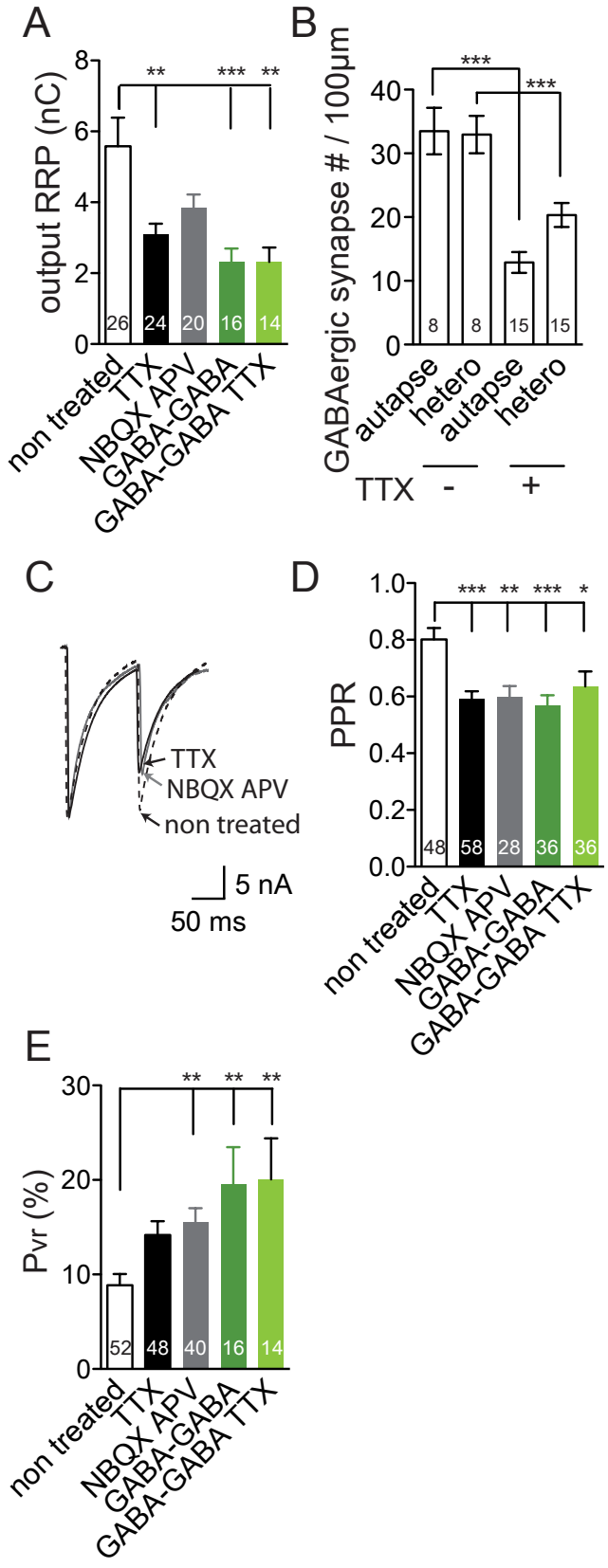
A
output RRP (nC)
8
6
4
2
0
**
***
**
26
24
20
16
14
non treated
TTX
NBQX APV
GABA-GABA
GABA-GABA TTX
B
GABAergic synapse # / 100µm
40
30
20
10
0
***
***
8
8
15
15
autapse
hetero
autapse
hetero
TTX
-
+
C
TTX
NBQX APV
non treated
5 nA
50 ms
D
PPR
1.0
0.8
0.6
0.4
0.2
0.0
***
**
***
*
48
58
28
36
36
non treated
TTX
NBQX APV
GABA-GABA
GABA-GABA TTX
E
Pvr (%)
30
20
10
0
**
**
**
52
48
40
16
14
non treated
TTX
NBQX APV
GABA-GABA
GABA-GABA TTX

Figure IIIA.4 Activity modulates GABAergic synapse properties in glu-GABA pair.

(A) Bar graph showing the mean GABAergic output RRP charges measured in glu-GABA pairs without (white) and with TTX (black) or NBQX/APV (grey) treatment and in untreated GABA-GABA pairs (green). $^{**}p \leq 0.01$. (B) Bar graph showing the mean GABAergic synapse density (number of synapses per 100 μm of dendritic length) of autapses and heterosynapses in glu-GABA pairs without and with TTX treatment. $^{***}p \leq 0.001$. (C) Representative paired-pulse IPSC traces recorded from glutamatergic neurons in untreated (dash), TTX-treated (black) and NBQX/APV-treated (grey) glu-GABA pairs. (D, E) Bar graph showing the mean values of GABAergic PPR (D) and P_{vr} (E) measured in glu-GABA pairs without and with TTX or NBQX/APV treatment and untreated in GABA-GABA pairs. $^{*}p \leq 0.05$; $^{**}p \leq 0.01$; $^{***}p \leq 0.001$. All values are mean ± SEM. Numbers in bar graphs are n values.

Neuronal activity is required for the modulation of glutamatergic input onto GABAergic neurons in glu-GABA pairs

Next we determined whether postsynaptic response properties were also altered in glu-GABA pairs. We examined miniature postsynaptic currents (mPSCs), which provide insight into postsynaptic receptor density and composition. Autaptic mEPSCs responses in glu-GABA pairs were similar to mEPSCs in glu-glu pairs (25.72±1.5 pA and 24.6±1.6 pA, respectively; $p = 0.36$). However, mEPSCs onto GABAergic neurons showed significantly increased amplitudes (Fig. IIIA.5A, 5B) and faster decay kinetics (1.9±0.1 ms, n=19 compared to mEPSC onto glutamatergic neurons 3.4±0.2 ms, n=21; $p < 0.0001$), effects that could be due to a different AMPA receptor composition in GABAergic neurons, presumably including the GluA2-lacking AMPA receptor (Geiger et al., 1997). The mIPSCs in glu-GABA pairs were similar in amplitude and decay time constant regardless of the postsynaptic neuron identity (autaptic: 41.8 ± 5.4 pA; heterosynaptic: 37.9 ± 4.3 pA). We also did not observe a change in mIPSC decay time constant (data not shown).

Interneurons have been shown to express GluA2-lacking AMPA receptors *in situ* (Geiger et al., 1995; Isaac et al., 2007). However, it is undetermined whether this is due to a cell autonomous program that is set up in early development or whether it is neuronal activity dependent. To test this, we studied the effect of chronic activity blockade on glutamatergic input onto GABAergic neurons in our two-cell culture system. TTX treatment (DIV 6-12) led to a significant decrease of mEPSC amplitudes onto GABAergic neurons (Fig. 5A) and slowing of the mEPSC decay time constant (non-treated: 1.9±0.1 ms; TTX: 3.4±0.3 ms; $p= 0.0005$), reaching values similar to those seen in the other glutamatergic synapses, which argues for a change in AMPA receptor composition. However, blocking ionotropic glutamate receptors did not change the properties of mEPSCs onto GABAergic neurons (Fig, IIIA.5A). Thus, glutamatergic input modifies postsynaptic glutamate responses in GABAergic neurons in an activity-dependent manner, which requires action potential (AP) generation. In contrast, autaptic mEPSCs in glu-GABA pairs were not affected by neuronal activity blockade with TTX or ionotropic glutamate receptor antagonist treatment (Fig. IIIA.5A), nor were mIPSC amplitudes of either synapse type (autaptic: 37.4 ± 1.8 pA; heterosynaptic: 43.4 ± 2.5 pA). The lack of change in autaptic mEPSC amplitude with

activity blockade suggests our two-cell culture system is lacking homeostatic synaptic plasticity (Turrigiano et al., 1998; Turrigiano and Nelson, 2004).

Synapses containing GluA2-lacking AMPA receptors exhibit inwardly rectifying postsynaptic responses (Jonas and Burnashev, 1995). Therefore, in order to further characterize the differences in AMPA receptor composition on GABAergic and glutamatergic neurons, we compared EPSC rectification in glu-glu and glu-GABA pairs. In glu-glu pairs, the EPSC in glutamatergic neurons exhibited a linear current-to-voltage relationship (Fig. IIIA.5C). In glu-GABA pairs, the EPSC in GABAergic neurons was partially inward rectifying (Fig. IIIA.5D) indicating the expression of GluA2-lacking AMPA receptors on GABAergic neurons. This rectification was abolished when neuronal activity was blocked by TTX treatment but not by ionotropic glutamate receptor antagonists, NBQX/APV (Fig. IIIA.5D). Therefore, these data indicate that neuronal activity but not the activation of ionotropic glutamate receptor shapes the GABAergic neuron's response to glutamatergic input.

Further analysis of the mPSC events revealed that mEPSC frequency (in glu-GABA pairs) was unchanged by pharmacological treatment (TTX: 11.2±1.3 Hz, n=20; no TTX: 15.1±1.8 Hz, n=19, p = 0.08), but, analogous to the modification of RRP size, the frequency of mIPSCs was significantly reduced in the TTX treated group (TTX: 5.1±0.8 Hz, n=22; no TTX: 9.1±1.4 Hz, n=22, p = 0.01).

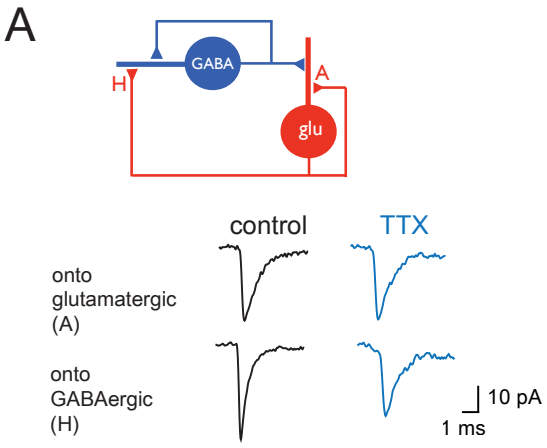
A
GABA
H
A
glu
control
TTX
onto
glutamatergic
(A)
onto
GABAergic
(H)
10 pA
1 ms

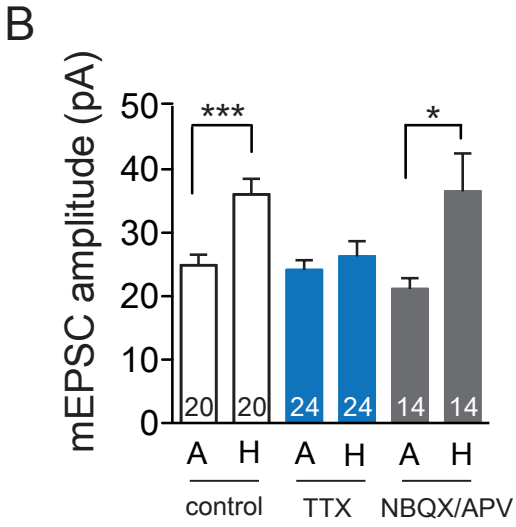
B
mEPSC amplitude (pA)
50
40
30
20
10
0
***
*
20
20
24
24
14
14
A
H
A
H
A
H
control
TTX
NBQX/APV

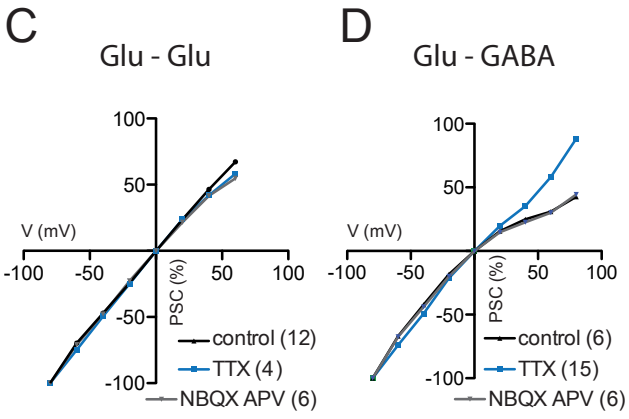
C
Glu - Glu
D
Glu - GABA
100
50
-50
-100
V (mV)
-100
-50
50
100
PSC (%)
control (12)
TTX (4)
NBQX APV (6)
control (6)
TTX (15)
NBQX APV (6)

Figure IIIA.5 Activity-dependent modulation of glutamatergic input onto GABA neurons. (A) Representative traces of mEPSCs recorded from glutamatergic (A: glutamatergic autapse; top) and GABAergic (H: glutamatergic heterosynapse; bottom) neurons without TTX (control, black) and with TTX (blue) treatment. (B) Bar graph showing the mean mEPSC amplitudes measured in glutamatergic (A) and GABAergic (H) neurons in glu-GABA pairs without and with TTX or NBQX/APV (grey) treatment. $^{*}p \leq 0.05$; $^{***}p \leq 0.001$. (C) Current-to-voltage relationship of the heterosynaptic connection in glu-glu pairs without (control) and with TTX or NBQX/APV treatment. (D) Same as (C) with the glutamatergic heterosynaptic connection to GABAergic neurons in glu-GABA pairs. All values are mean ± SEM. Numbers in bar graphs are n values.

Glutamatergic neuronal activity is required for the modulation of GABAergic synapse formation and function

As described above, inhibition of global neuronal activity resulted in a decreased GABAergic synapse number along with increased synaptic efficiency in our two-neuron microcircuit. We aimed to study which cell that's activity is required to modulate GABAergic synaptic properties. By taking the advantage of our two-neuron culture system, we suppressed either glutamatergic or GABAergic neuronal activity by cell type specific overexpression of the inward rectifying potassium channel, Kir2.1 (see Materials and Methods; (Burrone et al., 2002)). Then we examined the GABAergic synaptic output and input properties. Consistent with previous studies (Burrone et al., 2002), Kir2.1 expressing cells showed an inwardly rectifying current-to-voltage relationship (data not shown), reduced input resistance (37% and 27% decrease in glutamatergic and GABAergic neurons, respectively) and a hyperpolarized resting membrane potential compared to control cells (-20mV relative to the control).

We found that if Kir2.1-expressing cells were glutamatergic, the GABAergic output RRP sizes were significantly reduced compared to the control group (Fig. IIIA.6A). Consistent with our findings in Figure 4, reduced GABAergic RRP sizes exhibited increased synaptic efficiency, as indicated by a reduced PPR (Fig. IIIA.6B). However, these changes were not observed in pairs with a Kir2.1-expressing GABAergic neuron (Fig. IIIA.6A, B). Importantly, the glutamatergic neurons showed no change in output RRP or PPR regardless of whether they or the GABAergic neuron in the pair expressed Kir2.1 (output RRP: ctl 1.1 ± 1.3 nC, Kir2.1 in glu 1.1 ± 0.3 nC; p = 0.99; ctl 1.0 ± 0.2 nC, Kir2.1 in GABA 1.3 ± 0.2 nC; p = 0.28. PPR: ctl 1.4 ± 0.1, Kir2.1 in glu 1.4± 0.1; p = 0.77; ctl 1.1 ± 0, Kir2.1 in GABA 1.3 ± 0.1; p = 0.08).

Furthermore, in glutamatergic Kir2.1-expressing glu-GABA pairs the mEPSCs recorded in GABAergic neurons had strongly reduced amplitude compared to the equivalent connection in control glu-GABA pairs, while the autaptic mEPSC were not affected by Kir2.1 expression (Fig. IIIA.6C). Additionally, the difference in decay time of mEPSCs on GABAergic neurons compared to mEPSCs on glutamatergic neurons was abolished in glutamatergic Kir2.1-expressing glu-GABA pairs (decay time constant: control glu autapse: 3.5 ± 0.1 ms, n=16; control glu heterosynapse: 2.7 ± 0.2 ms,

n=15; p = 0.0004; Kir2.1 glu autapse: 3.4 ± 0.1 ms, n=15; Kir2.1 glu heterosynapse: 3.1 ± 0.3 ms, n=14; p = 0.31). However, in GABAergic Kir2.1–expressing glu-GABA pairs, the mEPSCs onto GABAergic or glutamatergic neurons were comparable to their respective group in control glu-GABA pairs (Fig. IIIA.6D). Therefore, these data indicate that in glu-GABA pairs the output, such as RRP size and vesicle release efficiency, from and the synaptic input onto the GABAergic neuron are shaped by activity of the glutamatergic neuron.

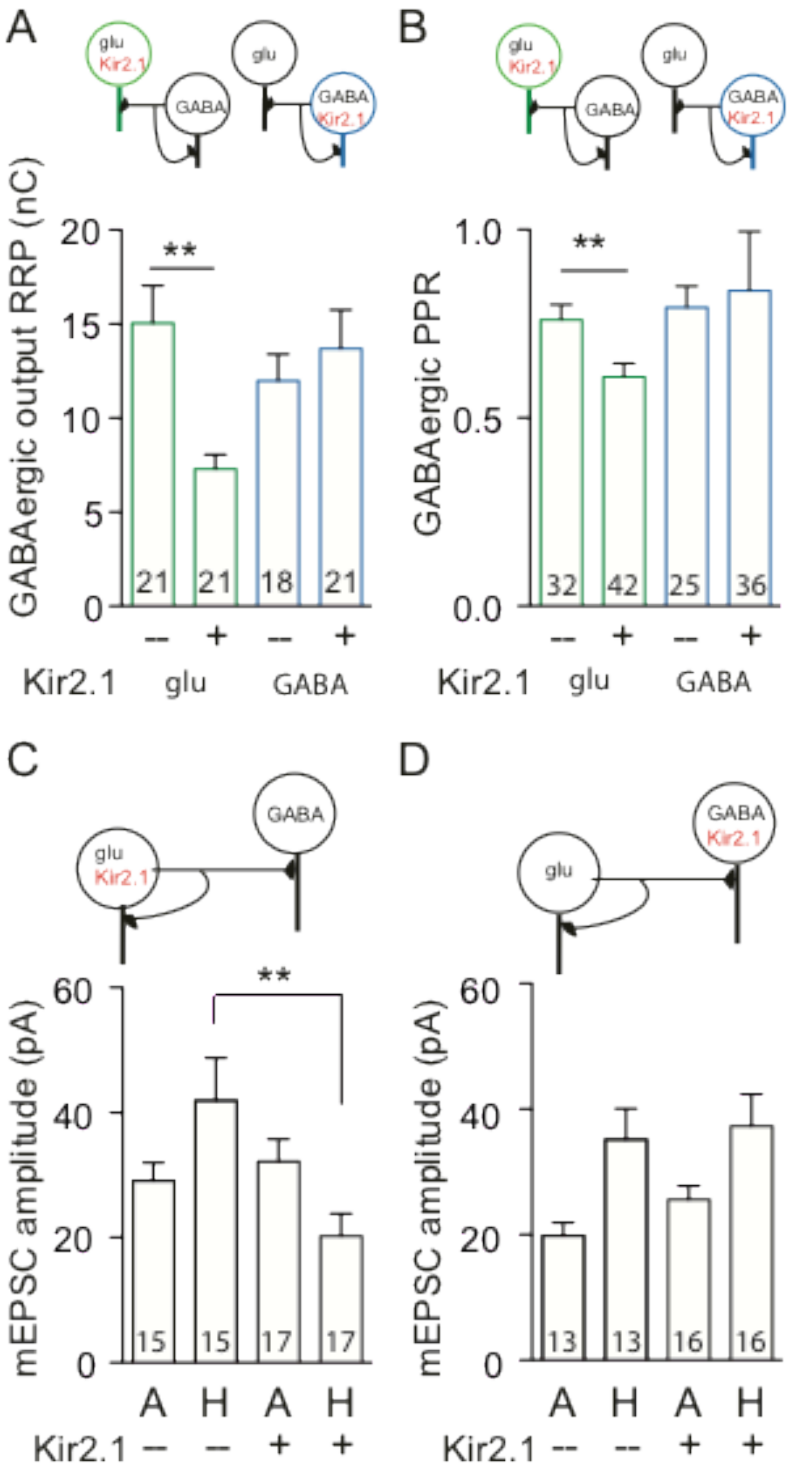
A
glu
Kir2.1
GABA
glu
GABA
Kir2.1
GABAergic output RRP (nC)
20
15
10
5
0
**
21
21
18
21
–
+
–
+
Kir2.1
glu
GABA
B
glu
Kir2.1
GABA
glu
GABA
Kir2.1
GABAergic PPR
1.0
0.5
0.0
**
32
42
25
36
–
+
–
+
Kir2.1
glu
GABA
C
GABA
glu
Kir2.1
mEPSC amplitude (pA)
60
40
20
0
**
15
15
17
17
A
H
A
H
Kir2.1
–
–
+
+
D
GABA
Kir2.1
glu
mEPSC amplitude (pA)
60
40
20
0
13
13
16
16
A
H
A
H
Kir2.1
–
–
+
+

Figure IIIA.6 Suppression of glutamatergic neuronal activity by Kir2.1 expression modulates GABAergic input and output in glu-GABA pairs. (A, B) Bar graphs showing the mean GABAergic output RRP charges (A; red connection in scheme) and PPR (B) with either a Kir2.1 expressing (+) or a control vector infected (-) glutamatergic (green) or GABAergic (blue) neuron. $^{**}p \leq 0.01$. (C) Bar graph showing the mean values of mEPSC amplitudes measured in glutamatergic (A) or GABAergic (H) neurons in glu-GABA pair with a Kir2.1 expressing (+) or control vector infected (-) glutamatergic cell. $^{*}p \leq 0.05$; $^{**}p \leq 0.01$. (D) Bar graph showing the mean values of mEPSC amplitudes measured in glutamatergic (A) or GABAergic (H) neurons in glu-GABA pair with a Kir2.1 expressing (+) or control vector infected (-) GABAergic cell. $^{*}p \leq 0.05$; $^{**}p \leq 0.01$. All values are mean ± SEM. Numbers in bar graphs are n values.

Part B

Basic properties of synapses in pairs of neurons

Before utilizing mixed cultures from wild type (WT) and mutant tissue, we examined basic properties of synaptic connections between pairs of WT glutamatergic neurons in comparison to autaptic connections from single WT neurons (Fig. IIIB.1A). In paired recordings we stimulated action potential induced EPSCs sequentially from both neurons and analyzed the responses at all four principal connections (Fig. IIIB. 1B).

The output EPSC amplitude defined as the sum of a neuron's evoked response onto itself (autaptic) and onto the second neuron (heterosynaptic), was nearly identical in size to the autaptic EPSC amplitude measured from single neurons (mean output EPSC amplitude, 4.7±0.6 nA; mean autaptic EPSC amplitude, 4.6±0.6 nA; Fig. IIIB.1C). Using pulsed application of 500 mOsm hypertonic solutions, we also determined the input RRP, representing all fusion competent vesicles from incoming synapses contacting to a single postsynaptic neuron (Fig. IIIB.1B). The input RRP size was comparable to the RRP size from single neuron cultures (mean input RRP charge, 633 ± 98 pC; mean autaptic RRP charge, 602 ± 95 pC; Fig. IIIB.1C). We calculated the input vesicular release probability (P_{vr}) by dividing input EPSC charge by input RRP charge, and the computed mean input P_{vr} value was similar to the P_{vr} of single autaptic neurons (mean input P_{vr}: 5.9±0.5 %; mean autaptic P_{vr}: 6.7±0.7 %; Fig. IIIB.1C). Thus, synaptic output or mean vesicle release probability of a cultured glutamatergic neuron does not further change upon addition of a second glutamatergic neuron.

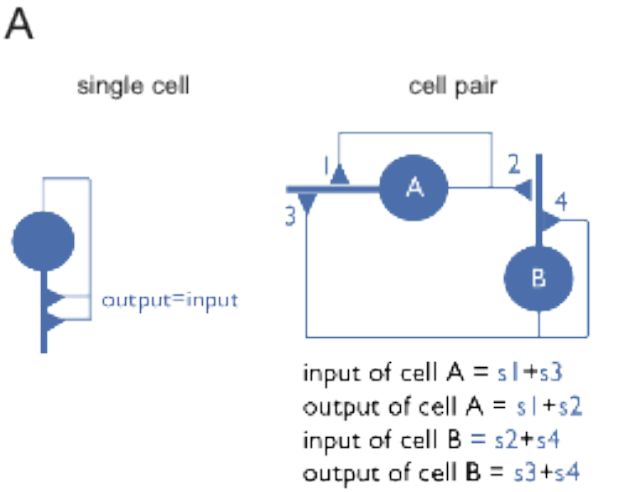
A
single cell
cell pair
output=input
1
2
3
4
A
B
input of cell A = s1+s3
output of cell A = s1+s2
input of cell B = s2+s4
output of cell B = s3+s4

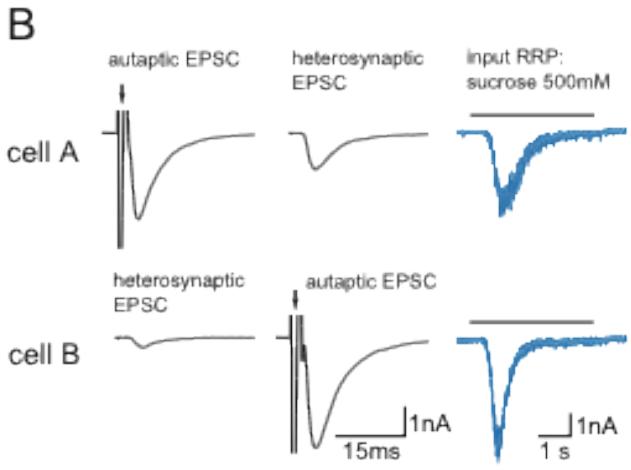
B
autaptic EPSC
heterosynaptic EPSC
input RRP: sucrose 500mM
cell A
heterosynaptic EPSC
autaptic EPSC
cell B
1nA
15ms
1nA
1 s

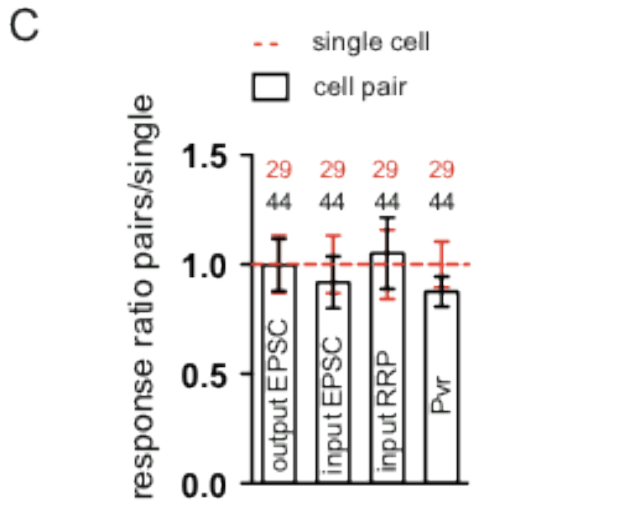
C
single cell
cell pair
response ratio pairs/single
1.5
1.0
0.5
0.0
29
44
29
44
29
44
29
44
output EPSC
input EPSC
input RRP
Pvr

Figure IIIB.1 Synaptic properties of autapses and heterosynapses in single and two-neuron cultures. (A) Schematic diagrams of a single and a two-neuron circuit illustrating the autaptic and heterosynaptic connections, the output excitatory postsynaptic current (output EPSCs), input EPSC and the input readily releasable pool (input RRP). (B) Current recordings from a pair of glutamatergic neurons. An action potential is evoked (arrow) in cell A leading to an autaptic response and a heterosynaptic response in cell B. After 2 s, an action potential is evoked in cell B leading to reciprocal responses. The colored traces correspond to the colored box in a larger scale. After another 3 s, hypertonic sucrose solution is applied for 4 s, which probes the input RRP response in both cells (blue traces). (C) Bar graph comparing the output and input EPSC, input RRP and vesicular release probability (P_{vr}) responses from pairs and single autaptic glutamatergic neurons by normalizing their responses to the corresponding single neuron recordings (mean ± SEM). Output EPSCs were calculated by adding the autaptic and heterosynaptic EPSC amplitudes evoked by an individual presynaptic neuron. Input EPSCs were calculated by adding the autaptic and the reciprocal heterosynaptic EPSC amplitudes. Input P_{vr} was defined as the input RRP released per input EPSC charge. The number of pairs/cells (black/red) recorded is indicated in the graph.

Loss of MeCP2 impairs synaptic output but not input

From previous work in single autaptic glutamatergic neurons, we know that MeCP2 deficiency led to half the number of glutamatergic synapses and evoked EPSC amplitude; while two-fold MeCP2 overexpression showed double the synapse number and EPSC amplitude (Chao et al., 2007). It is currently unclear from these experiments whether the rate limiting regulation of synapse number is determined at the pre- or postsynaptic site. Therefore, we used WT/MeCP2 mutant pairs to address this question. Two possible scenarios exist: if MeCP2 regulates a set of rate limiting factors at the postsynaptic site, synaptic input onto MeCP2 mutant neuron would be affected. It can be examined by comparing the input RRP and input spontaneous release frequency between the MeCP2 mutant neuron and wild type neuron. On the other hand, if MeCP2 has a rate limiting effect at the presynaptic site, synaptic output from MeCP2 mutant neuron would be affected. It can be examined by comparing the size of the output EPSC from the MeCP2 mutant neuron to the partner wild type neuron. We paired glutamatergic neurons from WT mice with neurons from MeCP2 mutant mice, which either express no MeCP2 (MeCP2-KO) or twice as much as wild type (MeCP2-overexpressing) (see Methods). We examined synaptic input and output EPSC as well as input RRP from each pair of WT/MeCP2-mutant neurons on a microisland.

In WT/MeCP2-KO neuron pairs, mutant neurons showed a nearly two-fold smaller output EPSC amplitude (Fig. 2B; $p < 0.01$, unpaired two-tail *t* test) but showed no change in input EPSC amplitude (Fig. IIIB.2C) and input RRP size (Fig. IIIB.2D). In WT/MeCP2-overexpressing neuron pairs, mutant neurons displayed a 1.5 fold larger output EPSC amplitude than wild type neurons (Fig. IIIB.3B; $p < 0.01$, unpaired two-tail *t* test); while input EPSC amplitude (Fig. IIIB.3C) and the size of input RRP (Fig. IIIB.3D) again did not show significantly difference between the two neurons. These data clearly demonstrate that MeCP2 levels regulate synaptic output, presumably through limiting a set of presynaptic factors that regulate synapse numbers.

The interaction between MeCP2 mutant and wild type neurons does not affect presynaptic release efficiency

While changes in MeCP2 expression do not affect release efficacy under the cell autonomous condition of single cell autaptic cultures, it remains to be determined

whether this also holds true in networks with mixed wild type and mutant neurons, as the MeCP2 deficiency is mosaic in RTT female patients. Indeed, measurements from MeCP2 deficient brain slices display profoundly altered short-term and long-term plasticity changes (Asaka et al., 2006), and alteration in synaptic output may influence target specificity. Therefore, we addressed the question of modulation of short-term plasticity and target specificity question in the mixed two-neuron network preparation.

We computed the presynaptic P_{vr} by comparing the input EPSC charge and the input RRP charge of WT or MeCP2 mutant neuron. The mean input P_{vr} measurement in wild type and mutant mixed pairs showed no difference (Fig. IIIB.2E and IIIB.3E). Since the input P_{vr} does not distinguish between wild type and mutant synapses, we compared paired-pulse rarios (PPRs) of each of the 4 connections, as this parameter is an excellent predictor for release efficiency (Fig. IIIB.4A). In both mixed WT/MeCP2-KO and WT/MeCP2-overexpressing mutant pairs, PPRs from MeCP2 mutant neurons was no significant different compare to the partner wild type neurons (Fig. IIIB.4B and IIIB.4C). In addition, we did not observe differences in PPRs between autaptic and heterosynaptic connections both in wild type and MeCP2 mutant neurons (Fig. IIIB.4B and IIIB.4C).

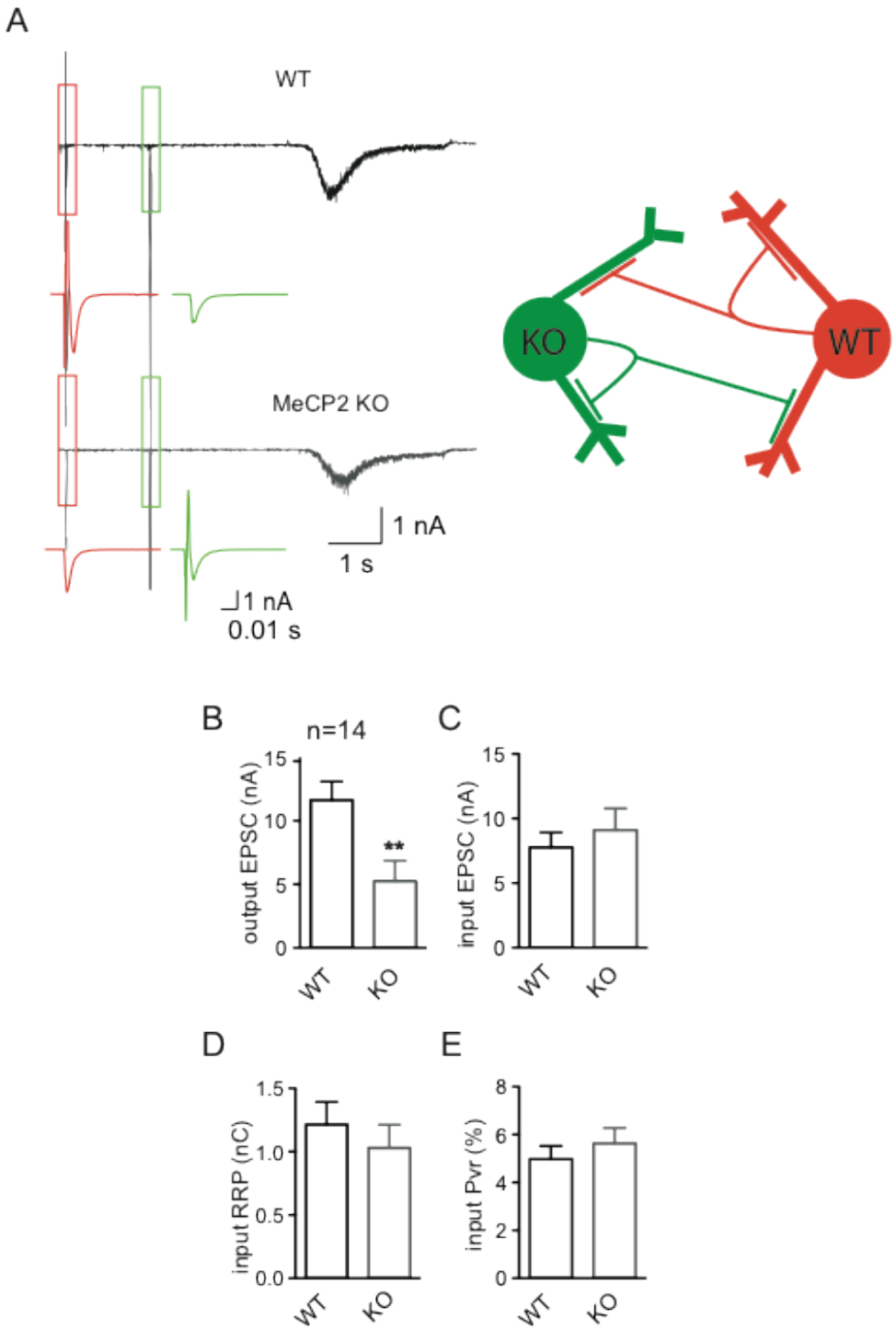
A
WT
MeCP2 KO
1 nA
1 s
1 nA
0.01 s
KO
WT
B
n=14
output EPSC (nA)
15
10
5
0
**
WT
KO
C
input EPSC (nA)
15
10
5
0
WT
KO
D
input RRP (nC)
1.5
1.0
0.5
0.0
WT
KO
E
input Pvr (%)
8
6
4
2
0
WT
KO

Figure IIIB.2 Synaptic properties of wild type and MeCp2 KO neurons in two-neuron cultures.

(A) Current recordings from a pair of wild type (black trace) and MeCP2 KO (grey trace) neurons. (B) Bar graphs show mean output EPSC amplitude from wild type (black bar) and MeCP2-KO (grey bar) neuron pair. Number of paired neuron analyzed (n) show on the top. (C) Bar graphs show mean input EPSC amplitude. (D) Bar graphs show mean input RRP. (E) Bar graphs show mean input P_{vr}.

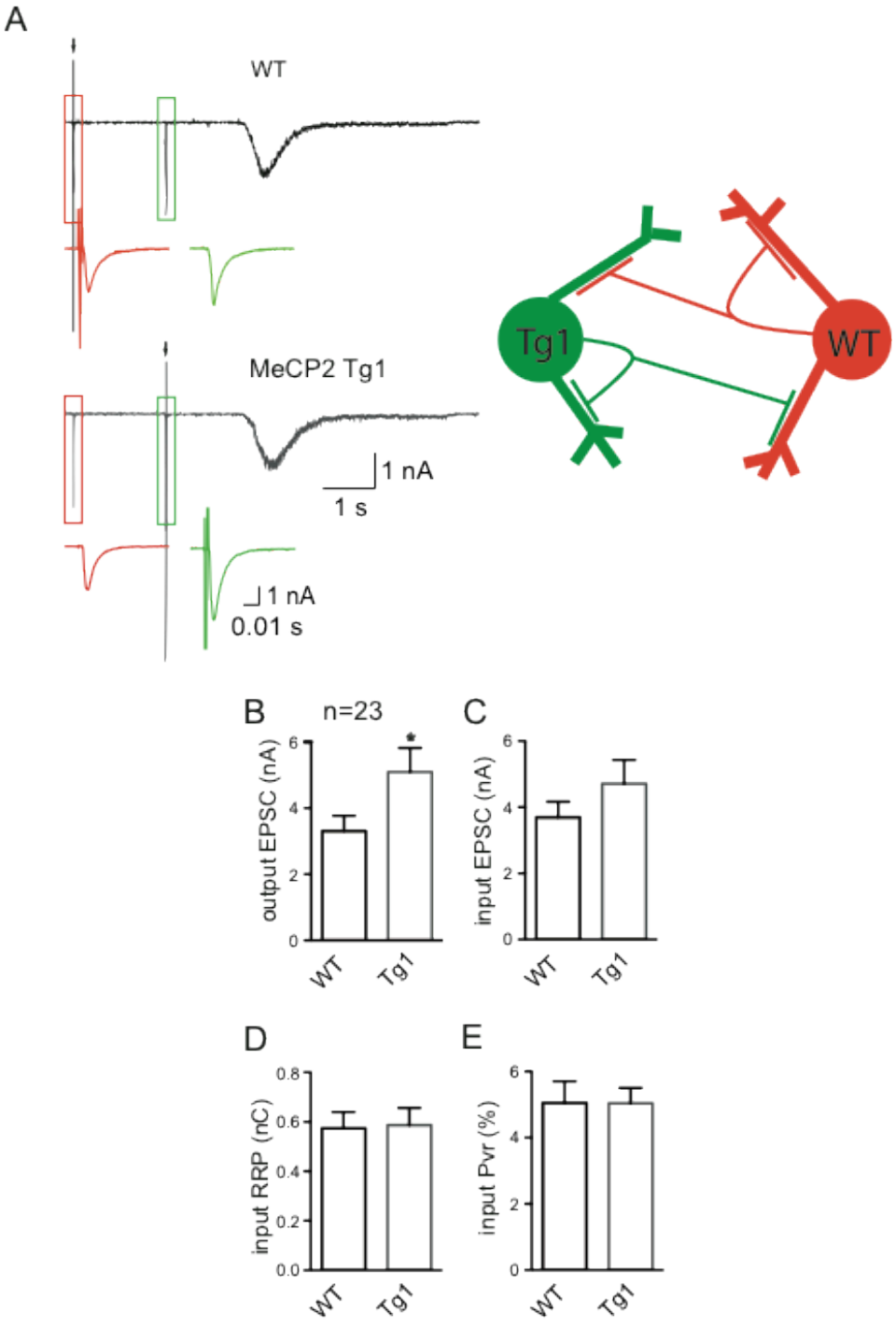
A
WT
MeCP2 Tg1
1 nA
1 s
1 nA
0.01 s
Tg1
WT
B
n=23
output EPSC (nA)
WT
Tg1
C
input EPSC (nA)
WT
Tg1
D
input RRP (nC)
WT
Tg1
E
input Pvr (%)
WT
Tg1

Figure IIIB.3 Synaptic properties of wild type and MeCP2 Tg1 neurons in two-neuron cultures.

(A) Current recordings from a pair of wild type (upper trace) and MeCP2 Tg1 (lower trace) neurons. (B) Bar graphs show mean output EPSC amplitude from wild type and MeCP2 Tg1 neuron pair. Number of paired neuron analyzed (n) shown in the top. (C) Bar graphs show mean input EPSC amplitude. (D) Bar graphs show mean input RRP. (E) Bar graphs show mean input P_{vr}.

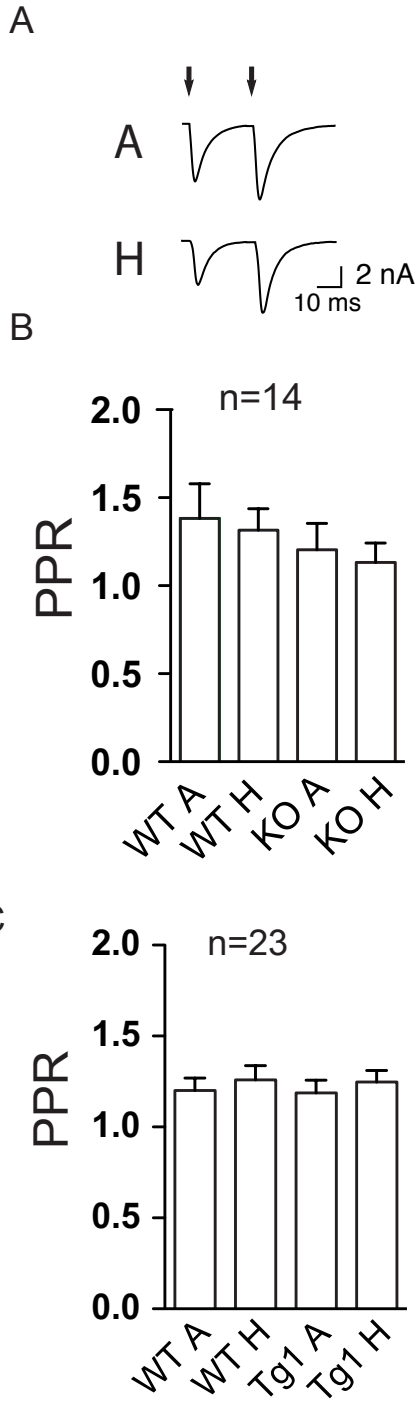
A
A
H
2 nA
10 ms
B
n=14
PPR
2.0
1.5
1.0
0.5
0.0
WT A
WT H
KO A
KO H
C
n=23
PPR
2.0
1.5
1.0
0.5
0.0
WT A
WT H
Tg1 A
Tg1 H

Fig. IIIB.4 PPRs of synaptic connections in wild type and MeCP2 mutant two-neuron circuit. (A) Upper, representative autaptic (A) and heterosynaptic (H) current traces from a pair of neurons stimulated under a paired pulse stimulation regime (interval 25 ms). Depolarization artifact and action potential are blanked. Bottom. Bar graphs show autaptic and heterosynaptic EPSC paired-pulse ratios (PPRs) from neuronal pairs and autaptic PPRs from single-neuron recordings (mean ± SEM). Numbers of pairs/cells are shown in the graph. (B) and (C), Bar graph of autaptic and heterosynaptic EPSC paired-pulse ratios (PPRs) from wild type and MeCP2-KO or WT and MeCP2-Tg1 neuronal pairs (mean ± SEM).

Chapter IV

Conclusion, Discussion and Future Direction

A. Investigation of synapse formation and function in glutamatergic-GABAergic two-neuron microculture

Precise balance between excitatory and inhibitory activity is critical for proper information processing. Functional impairment in either excitation or inhibition may affect the overall synaptic connection and properties in the neuronal circuit, therefore leads to neurological disorder such as seizure, Rett syndrome, autisms and Down syndrome (Dani et al., 2005; Kuzirian and Paradis, 2011; Banerjee et al., 2012). Hence, elucidating the basic rules that govern excitatory and inhibitory synapse connections and functions is not only critical for understanding neuronal circuit formation but also may shed light onto the pathogenesis of the related neurological disorders.

In this dissertation (Chapter IIIA), we used the two-neuron microcircuit to investigate synaptic formation and function in a reduced network of glutamatergic and GABAergic neurons (Chapter IIIA). We show that in a glutamate-GABA microcircuit, while glutamatergic neurons remained insensitive to glutamatergic or GABAergic innervation, the GABAergic neurons exhibited modulation of both synaptic input and output properties in a manner consistent with GABAergic synapse maturation *in vivo* (Marty et al., 2000; Chattopadhyaya et al., 2004; Colin-Le Brun et al., 2004), which we show was due to glutamatergic input. GABAergic input modulation required AP firing of glutamatergic neurons, which led to a switch of postsynaptic AMPA receptor composition from linear to inward rectifying (Fig. IIIA.5). GABAergic output changed through an expansion of synapse number accompanied by reduced release efficacy (Fig. IIIA.2 and IIIA.3). Both AP firing of glutamatergic neurons and glutamate receptor activation were required to induce output modulation (Fig.IIIA.4 and IIIA.5). The changes initiated in the GABAergic neuron were cell-wide and not target cell specific with regard to neurotransmitter identity, possibly suggesting the activation of a different genetic program with excitatory input. To the contrary, no change in the synaptic output or input of the glutamatergic neuron regardless of partner or activity level suggests that this cell type's intrinsic program does not require input for activation.

1. Mechanism of output modulation

The emergence of glutamatergic input onto GABAergic neurons increased the number of GABAergic synapses but at the same time decreased their efficiency of release. Interestingly, both increased synaptogenesis (Marty et al., 2000; Chattopadhyaya et al., 2004; Colin-Le Brun et al., 2004) and decreased release probability (Morales et al., 2002; Jiang et al., 2005; Tang et al., 2007) have been reported separately as hallmarks of GABAergic neuron maturation in the developing hippocampus and cortex. The modulation we observed required AP firing and the activation of ionotropic glutamate receptors (Fig. IIIA.5). Chronic blockade of Ca^{2+} permeable AMPA receptors also impaired the GABAergic output modification (data not shown), although it is unclear whether this was due to impaired Ca^{2+} influx into the GABAergic neuron or reduced overall excitatory input. As for neuronal activity, expression of Kir2.1 in glutamatergic neurons alone reversed the GABAergic output properties, while expression of Kir2.1 in the GABAergic neuron did not. However, in the latter configuration, we still cannot rule out the possibility that the large input from the partner glutamatergic neuron in the microcircuit evokes firing in the GABAergic Kir2.1 neuron. Furthermore, we found that activity suppression in the glutamatergic neuron by Kir2.1 expression did not affect its own synapse formation and function, which is consistent with previous findings (Craig et al., 1994; Rao and Craig, 1997; Gomperts et al., 2000).

What is the mechanism for the reduced vesicle release probability accompanying the increased GABAergic synapse number? The simplest explanation may be that while making additional synapses requires the up regulation of hundreds of genes, gene products affecting synaptic output such as voltage-gated channels may not be up regulated proportionately leading to their dilution over more synapses. Alternatively, active mechanisms could explain this result. For example, presynaptic release probability changes, attributed to active Ca^{2+} modulation, are observed when postsynaptic excitability is altered in *Drosophila* neuromuscular junction (Paradis et al., 2001) or global network activity is blocked in culture (Zhao et al., 2011).

2. Postsynaptic modulation of glutamatergic input onto GABAergic neuron

Glutamatergic input is required for clustering AMPA receptors on hippocampal GABAergic neurons (Rao et al., 2000). We found that glutamatergic input also regulates the functional properties of these AMPA receptors. Glutamatergic responses in GABAergic neurons of the two-neuron microcircuit show inward rectification, large mEPSC amplitudes and faster decay kinetics (Fig. IIIA.5), which is reminiscent of the GluA2-lacking AMPA receptor composition often observed in GABAergic neurons (McBain and Dingledine, 1993; Geiger et al., 1995; Isa et al., 1996; Racca et al., 1996; Liu and Cull-Candy, 2000). However, when AP firing in glutamatergic neurons was impeded, the AMPA receptor responses in GABAergic neurons showed characteristics of GluA2-containing AMPA receptors (Fig. IIIA.6). We suggest that the default AMPA receptor composition of synapses on GABAergic neurons is GluA2-containing, and incorporation of GluA2-lacking AMPA receptors depends on glutamatergic neuronal activity and synaptic contact. The transition from Ca^{2+} impermeable to Ca^{2+} permeable AMPA receptors on GABAergic neurons following glutamatergic innervation may mark a step in maturation of the GABAergic neuron. This is in contrast to more dynamic activity-dependent modification of AMPA receptor composition, such as at the parallel fiber to stellate cell synapse in cerebellum, where high frequency stimulation converts rectifying receptors to linearly conducting receptors (Liu and Cull-Candy, 2000; Liu and Cull-Candy, 2002).

Interestingly, ionotropic glutamate receptor antagonists did not prevent the incorporation of GluA2-lacking receptors into synapses on the GABAergic neurons. Thus, initial synaptic contact together with AP firing in the glutamatergic neuron is sufficient for incorporation of inward rectifying receptors. This result suggests that activity-dependent signals from glutamatergic neurons, such as AP-dependent release of trophic factors, might induce the expression of GluA2-lacking AMPA receptors on the GABAergic neuron, as has been suggested to occur in glutamatergic neurons (Nakata and Nakamura, 2007; Fortin et al., 2012).

3. Cell autonomous regulation in two-neuron culture system

The properties of *in vivo* circuits are the result of intrinsic cellular programs and extrinsic network effects. In our reduced network environment, we suggest that

glutamatergic neurons behave in a cell intrinsic fashion; they showed no change in synapse formation or function when cells received inputs from either glutamatergic or GABAergic neurons or experienced changes in activity levels (Fig. IIIA.1-3). As further evidence of cell intrinsic behavior, we found that the total number of synapses an individual glutamatergic neuron makes is not different between single and paired neurons. These results suggest that the glutamatergic neuron may be programmed to form a fixed number of connections, which is consistent with previous findings for glutamatergic neurons in microcircuit (Mennerick et al., 1995) and mass culture preparations (Harms et al., 2005). Impeding AP firing in a postsynaptic neuron was shown to result in a decrease in glutamatergic synaptic contacts onto that neuron with respect to other neurons in the network (Burrone et al., 2002). However, global activity blockade does not result in a decrease in glutamatergic synapse formation (Craig et al., 1994; Rao and Craig, 1997; Gomperts et al., 2000; Burrone et al., 2002; Wierenga et al., 2006; Lu et al., 2013), suggesting the effect of a postsynaptic neuron's activity on synaptic density is network dependent.

In the traditional sense, the changes induced in GABAergic neurons in response to glutamatergic innervation are not cell autonomous in nature. It has been shown that silencing neuronal activity inhibits the formation of GABA synapses in a network-dependent fashion (Marty et al., 2000; Hartman et al., 2006). Consistent with these results, we found that the modulation of GABAergic input and output required the activity of a glutamatergic neuron (Fig. IIIA.6). Additionally, we interpret these changes as a maturational switch between cellular programs by glutamatergic input, as the changes were cell wide and not target cell specific. Both autaptic and heterosynaptic synapses contacting different postsynaptic cell types exhibited the same synapse density and degree of decrease in synaptic release efficiency (Fig. IIIA.2 and IIIA.3). In more complex networks, extrinsic factors likely further influence these processes as synapse formation and short-term plasticity (Shigemoto et al., 1996; Thomson, 1997; Reyes et al., 1998; Scanziani et al., 1998; Gupta et al., 2000; Toth and McBain, 2000; Fioravante and Regehr, 2011) exhibit target cell specificity

4. Homeostatic plasticity in two-neuron microcircuit

Synaptic scaling is one type of the synaptic modifications involved in homeostatic plasticity. It has been suggested that homeostatic scaling induced by activity blockade during synapse development (DIV 6-12) (Turrigiano et al., 1998; Burrone et al., 2002; Hartman et al., 2006; Wierenga et al., 2006). However, we did not observe changes in the amplitude of mPSCs either for glutamatergic or GABAergic synapses after blockade of neuronal activity during synapse formation in our two-neuron culture system (Fig. IIIA. 5B and data not shown). The lack of synaptic scaling in the two-neuron culture system may suggest that the network effects play a role in homeostatic regulation of synaptic scaling.

In addition, several studies have shown that different forms of homeostatic plasticity can be induced at different developmental stages of the hippocampal and cortical neurons (Burrone et al., 2002; Wierenga et al., 2006). In younger cortical neuron cultures (≤ 14 DIV), global activity blockade for 2 days increases the amplitude of mEPSCs without affecting mEPSC frequency. However, global activity blockade for 2 days in older cultures (≥ 18DIV) induces an increase in mEPSC frequency, without affecting mEPSC amplitude (Wierenga et al., 2006). Therefore, to test in detail whether homeostatic plasticity exists in the two-neuron culture system, we could manipulate neuronal activity at different time points during development.

5. The types of hippocampal GABAergic neuron are highly diverse

In the study, we identified the cell types as glutamatergic and GABAergic by their functional properties and the expressions of marker proteins. However, in vivo, there are diverse types of GABAergic interneurons in the hippocampus (McBain and Fisahn, 2001; Somogyi and Klausberger, 2005). Interneurons can be broadly classified into fast spiking versus non-fast-spiking and soma inhibiting versus dendrite-inhibiting cells. Moreover, based on calcium binding proteins (such as parvalbumin, calretinin and calbindin) and neuropeptides (such as somatostatin and cholecystokinin), GABAergic neurons can be subdivided into large different sets (Freund and Buzsaki, 1996). At least two types of GABAergic neurons, namely fast spiking and non-fast spiking GABAergic neurons, have been identified in hippocampal autaptic culture system (Ikeda et al., 2008). Therefore, one of the future directions would be to categorize the

GABAergic synaptic modification by activity of either fast spiking or non-fast spiking GABAergic neurons. We could also subdivide the GABAergic neurons by neuropeptides or calcium-binding protein markers through *post hoc* immunocytochemistry.

6. Implications for network function

We have observed the increase of GABAergic neuron synapse formation and the decrease of its synaptic efficiency in response to glutamatergic innervations. These results would lead to several implications for the *in vivo* network functions.

In terms of the effect on synapse formation, consistent with others' findings (Marty et al., 2000; Chattopadhyaya et al., 2004; Colin-Le Brun et al., 2004; Hartman et al., 2006), excitatory input causes an increase in the number of synapses formed by ta GABAergic neuron; more postsynaptic neurons will therefore receive inhibition.

Related to the synaptic efficiency, release efficiency decrease with input activity during postnatal development, according to a previous study done in cortical neurons (Morales et al., 2002; Jiang et al., 2005; Tang et al., 2007). For example, the release probability of GABAergic neurons from visual cortex decrease during maturation (Jiang et al., 2005). Such a decrease in release probability during development has also been observed in GABAergic neurons of superior colliculus (Kirischuk et al., 2005; Grantyn et al., 2011). Since we have observed the synaptic efficiency of these synapses is decreased in parallel with increase of synapse number, we propose the inhibitory synaptic strength at a single contact in response to a single AP would appear weaker.

The plastic changes that we observed in GABAergic neurons during maturation suggest a higher spatial (synapse number increase) and better temporal inhibition (reduced PPD) to higher frequencies, possibly to control neuronal circuit excitability during dynamic information processing *in vivo*. However, glutamatergic neurons operate on a fixed cell intrinsic program that governs synapse formation (Lu et al., 2013) and function. These observations suggest a developmental orchestration between glutamatergic and GABAergic neurons for forming a mature neuronal network. Taken together, since GABAergic neuronal maturation appears to be preserved in the two-neuron microcircuit, this will serve as an excellent model for studying synapse formation and function in developing excitatory/inhibitory circuits.

B. MeCP2 controls glutamatergic presynapse formation

In the second part of my dissertation, we used two-neuron culture to identify the origin of the synapse formation deficit in MeCP2 mutant mice. I found that in mixed pair of wt/MeCP2-KO neuron pairs, MeCP2-KO neurons showed a decrease in output EPSC amplitude compared to wild type neurons. Input EPSC amplitudes and input RRP sizes were not affected. In wt/MeCP2-overexpressing neuron pairs, MeCP2-overexpressing neurons displayed an increase in output EPSC amplitude without affecting the input EPSC amplitude or the input RRP size compared to wild type neurons. Based on our hypothesis (Introduction, Figure H4a, H4b), these data clearly demonstrate that MeCP2 levels regulate output but not input synaptic strength. This data strongly suggests that MeCP2 regulates synapse formation through a set of presynaptic factors.

1. MeCP2 mutant neurons show defects in synaptic output but not input

In principle, the defect in synaptic function in individual neuron will eventually affect the complete neuronal network. This is exemplified by female (heterozygote) RTT patients, whose neurons have a mosaic pattern of wild type and MeCP2 mutant expression due to X-chromosome inactivation mutanted (Anvret and Wahlstrom, 1994; Amir et al., 2000). Two-neuron microcircuits made up of a wild type and MeCP2 mutant neuron can serve as a model for such patterns. We observed that the mutant neurons showed normal function in receiving input but failed to produce normal levels of output synaptic strength (Fig. IIIB.2-3). As a result, this might alter the fidelity of signal propagation in the neuronal network.

Consistent with a previous study using the autaptic culture system (Chao et al., 2007), the decrease in excitatory synaptic strength (Fig. IIIB.2B) in a MeCP2 deficient neuron paired with a wild type neuron was correlated to the decrease in it's synapse number (data not shown). Furthermore, we also did not observe changes in synaptic efficiency in MeCP2 KO and MeCP2 overexpression neurons compared to its partner wild type neuron (Fig. IIIB.4A and IIIB.4B) (Chao et al., 2007).

What is the possible mechanism responsible for the synaptic output deficits? It was previously shown that a lack of MeCP2 is associated with a decreased number of axons (Belichenko et al. 2009) and a defect in axon targeting (Belichenko et al., 2009;

Matarazzo et al., 2004). Therefore, one of the possible mechanisms contributing to the synaptic output deficiency that we observed in MeCP2 mutant neurons may be abnormal axon outgrowth. To verify this mechanism, further experiments are required.

C. Future directions

1. **Understanding the possible mechanisms responsible for modulation of GABAergic synapse formation by neuronal activity**

a. BDNF

We identify a cellular process where innervation of glutamatergic affects GABAergic synapse input and output. To search mechanisms, trophic factor BDNF is one of the candidates. BDNF can modulate GABAergic synapse properties (Hong et al., 2008). BDNF is released from glutamatergic neurons in an activity-dependent manner and it contributes to enhance GABAergic synapse formation (Huang et al., 1999; Marty et al., 2000; Seil and Drake-Baumann, 2000; Chattopadhyaya et al., 2004). To elucidate the possibility that BDNF is involved, one could knockout the BDNF receptors specifically on GABAergic neurons by overexpressing a target cell specific virus with siRNA targeting TrkB receptors and examine whether the GABAergic synapse formation is altered or not. Furthermore, in parallel, we could also examine whether synaptic efficiency, another output phenotype we observed, is affected by blocking the BDNF signals in GABAergic neurons.

b. Activity-dependent gene expression in GABAergic neuron

In response to alteration of neuronal activity, neurons regulate synaptic formation and function by changing the gene expression (Ebert et al 2013, West AE 2011). For example, activity-dependent release of excitatory neurotransmitters initiates membrane depolarization and calcium influx into the cytoplasm. Calcium influx-triggered calcium-dependent signaling events regulate the expression of transcription factors that coordinate genes expression involved in modulation of neuronal function (Cohen 2008; Zhang 2011; Flavell 2008). For example, *c-fos* is involved in regulating neuronal structure and function in CNS (Flavell et al., 2008; West and Greenberg 2011). In addition to transcription factors, it has been shown that Rem2, an activity dependent Ras-related small GTPase, regulates GABAergic synapse formation (Finlin

et al., 2005; Paradis et al., 2007). Knockout of Rem2 decreases the density of GABAergic synapses (Paradis et al., 2007). It will be interesting to examine the expression and activity of both reporters in GABAergic neurons that are innervated in glutamtergic or GABAergic neurons.

c. Activity-dependent gene expression in glutamatergic neuron

The synaptic modifications that we observed in GABAergic neurons required input activity from glutamatergic neurons and are cell-wide and non-cell type specific (Fig. IIIA.4 and IIIA.6). This suggests that the modification of GABAergic synapse formation may result from a change of activity-dependent gene expression by the postsynaptic neuron. A previous study has shown that Npas4, an activity-dependent transcription factor in glutamatergic neurons, is involved in GABAergic synapse formation onto glutamatergic neurons (Lin et al., 2008). The knockdown or overexpression of Npas4 decreases and increases the GABAergic synapse formation onto glutamatergic neurons, respectively (Lin et al., 2008). Another transcription factor, myocyte enhancer factor 2 (MEF2), has also been suggested to regulate GABAergic synapse formation because of its transcriptional regulation of *bdnf* (Hong et al., 2008; West and Greenberg 2011).

Taking together, future directions that focus on finding activity dependent genes either expressed in glutamatergic or GABAergic neurons should help us to elucidate the molecular mechanisms by which activity regulates the formation of GABAergic synapses. This data might provide some insights into how homeostatic balance is regulated between excitation and inhibition.

2. The role of glucocorticoid in MeCP2 mutation mediated synaptic dysfunction

Mutation in *MeCP2* causes neurological defects in CNS, which leads to RTT. In addition, MeCP2 also involves in modulation of glucocorticoid-system. Two glucocorticoid regulated gene products, glucocorticoid-inducible kinase (*Sgk1*) and FK506-binding protein 51 (*Fkbp5*), are up regulated in MeCP2-null mice (Nuber et al., 2005). Furthermore, MeCP2 acts as a transcriptional repressor for these two genes (Nuber et al., 2005). Therefore, these data indicate that MeCP2 might involve in the

negative regulation of glucocorticoid system. Importantly, glucocorticoid antagonist treatment rescues the neurological symptoms that have been seen in MeCP2-null mice (Braun et al., 2012).

In order to further study the casual role by glucocorticoid system in MeCP2 pathophysiology in nervous system, one could examine how glucocorticoid modulates the dysfunction of synaptic properties in a cell-autonomous manner that we observed in MeCP2 mutant neurons (Chao et al, 2007, Chao et al, 2010).

3. Excitation and inhibition in Rett syndrome

Imbalance between excitatory and inhibitory synaptic activities is considered to be one of the major consequences of MeCP2 deficiency in the neuronal network (Dani et al., 2005; Chao et al., 2010; Kuzirian and Paradis, 2011). Furthermore, the *MeCP2* gene is X-linked in mammals and can be inactivated in females; about 50 % of the cells in heterozygote females therefore have an inactivated *MeCP2* mutant allele (Anvret and Wahlstrom, 1994; Amir et al., 2000). Therefore, this mosaic expression of MeCP2 in either the excitatory or inhibitory neurons complicates the mechanisms that contribute to the deficits of neuronal function in the network.

In order to study the basic interaction between wild type and MeCP2 mutant neurons in circuits with excitation and inhibition, it will be interesting to apply the glu-GABA two-neuron culture system where one neuron is wild type and the other is MeCP2 mutant. Using the information we obtained on basic synaptic properties of circuit formation in glu-GABA two-neuron microculture, as our future direction, we hope to gain insight into the MeCP2 regulated mechanisms that cause imbalance of excitation and inhibition.

Bibliography

Albert H, Dale EC, Lee E, Ow DW (1995) Site-specific integration of DNA into wild-type and mutant lox sites placed in the plant genome. Plant J 7:649-659.

Amir RE, Van den Veyver IB, Wan M, Tran CQ, Francke U, Zoghbi HY (1999) Rett syndrome is caused by mutations in X-linked MECP2, encoding methyl-CpG-binding protein 2. Nat Genet 23:185-188.

Anvret M, Wahlstrom J (1994) Rett syndrome: random X chromosome inactivation. Clin Genet 45:274-275.

Araki K, Araki M, Yamamura K (1997) Targeted integration of DNA using mutant lox sites in embryonic stem cells. Nucleic Acids Res 25:868-872.

Asaka Y, Jugloff DG, Zhang L, Eubanks JH, Fitzsimonds RM (2006) Hippocampal synaptic plasticity is impaired in the Mecp2-null mouse model of Rett syndrome. Neurobiol Dis 21:217-227.

Basu J, Betz A, Brose N, Rosenmund C (2007) Munc13-1 C1 domain activation lowers the energy barrier for synaptic vesicle fusion. J Neurosci 27:1200-1210.

Baroncelli L, Braschi C, Spolidoro M, Begenisic T, Maffei L, Sale A (2011) Brain plasticity and disease: a matter of inhibition. Neural Plast 2011:286073.

Bekkers JM, Stevens CF (1991) Excitatory and inhibitory autaptic currents in isolated hippocampal neurons maintained in cell culture. Proc Natl Acad Sci U S A 88:7834-7838.

Belichenko PV, Wright EE, Belichenko NP, Masliah E, Li HH, Mobley WC, Francke U (2009) Widespread changes in dendritic and axonal morphology in Mecp2-mutant mouse models of Rett syndrome: evidence for disruption of neuronal networks. J Comp Neurol 514:240-258.

Braun S, Kottwitz D, Nuber UA (2012) Pharmacological interference with the glucocorticoid system influences symptoms and lifespan in a mouse model of Rett syndrome. Hum Mol Genet 21:1673-1680.

Burrone J, O'Byrne M, Murthy VN (2002) Multiple forms of synaptic plasticity triggered by selective suppression of activity in individual neurons. Nature 420:414-418.

Chahrour M, Zoghbi HY (2007) The story of Rett syndrome: from clinic to neurobiology. Neuron 56:422-437.

Chahrour M, Jung SY, Shaw C, Zhou X, Wong ST, Qin J, Zoghbi HY (2008) MeCP2, a key contributor to neurological disease, activates and represses transcription. Science 320:1224-1229.

Chang BS, Lowenstein DH (2003) Epilepsy. N Engl J Med 349:1257-1266.

Chao HT, Zoghbi HY, Rosenmund C (2007) MeCP2 controls excitatory synaptic strength by regulating glutamatergic synapse number. Neuron 56:58-65.

Chattopadhyaya B, Di Cristo G, Higashiyama H, Knott GW, Kuhlman SJ, Welker E, Huang ZJ (2004) Experience and activity-dependent maturation of perisomatic GABAergic innervation in primary visual cortex during a postnatal critical period. J Neurosci 24:9598-9611.

Chen RZ, Akbarian S, Tudor M, Jaenisch R (2001) Deficiency of methyl-CpG binding protein-2 in CNS neurons results in a Rett-like phenotype in mice. Nat Genet 27:327-331.

Cobos I, Calcagnotto ME, Vilaythong AJ, Thwin MT, Noebels JL, Baraban SC, Rubenstein JL (2005) Mice lacking Dlx1 show subtype-specific loss of interneurons, reduced inhibition and epilepsy. Nat Neurosci 8:1059-1068.

Cohen-Cory S (2002) The developing synapse: construction and modulation of synaptic structures and circuits. Science 298:770-776.

Colin-Le Brun I, Ferrand N, Caillard O, Tosetti P, Ben-Ari Y, Gaiarsa JL (2004) Spontaneous synaptic activity is required for the formation of functional GABAergic synapses in the developing rat hippocampus. J Physiol 559:129-139.

Collins AL, Levenson JM, Vilaythong AP, Richman R, Armstrong DL, Noebels JL, David Sweatt J, Zoghbi HY (2004) Mild overexpression of MeCP2 causes a progressive neurological disorder in mice. Hum Mol Genet 13:2679-2689.

Colon-Ramos DA (2009) Synapse formation in developing neural circuits. Curr Top Dev Biol 87:53-79.

Craig AM, Blackstone CD, Huganir RL, Banker G (1994) Selective clustering of glutamate and gamma-aminobutyric acid receptors opposite terminals releasing the corresponding neurotransmitters. Proc Natl Acad Sci U S A 91:12373-12377.

Dani VS, Nelson SB (2009) Intact long-term potentiation but reduced connectivity between neocortical layer 5 pyramidal neurons in a mouse model of Rett syndrome. J Neurosci 29:11263-11270.

Del Castillo J, Katz B (1954) Quantal components of the end-plate potential. J Physiol 124:560-573.

Deng JV, Rodriguiz RM, Hutchinson AN, Kim IH, Wetsel WC, West AE (2010) MeCP2 in the nucleus accumbens contributes to neural and behavioral responses to psychostimulants. Nat Neurosci 13:1128-1136.

Denker A, Rizzoli SO (2010) Synaptic vesicle pools: an update. Front Synaptic Neurosci 2:135. Denker A, Rizzoli SO (2010) Synaptic vesicle pools: an update. Front Synaptic Neurosci 2:135.

Dobrunz LE, Stevens CF (1997) Heterogeneity of release probability, facilitation, and depletion at central synapses. Neuron 18:995-1008.

Felmy F, Neher E, Schneggenburger R (2003) Probing the intracellular calcium sensitivity of transmitter release during synaptic facilitation. Neuron 37:801-811.

Fernandez F, Garner CC (2007) Over-inhibition: a model for developmental intellectual disability. Trends Neurosci 30:497-503.

Fioravante D, Regehr WG (2011) Short-term forms of presynaptic plasticity. Curr Opin Neurobiol 21:269-274.

Flavell SW, Greenberg ME (2008) Signaling mechanisms linking neuronal activity to gene expression and plasticity of the nervous system. Annu Rev Neurosci 31:563-590.

Fortin DA, Srivastava T, Dwarakanath D, Pierre P, Nygaard S, Derkach VA, Soderling TR (2012) Brain-derived neurotrophic factor activation of CaM-kinase kinase via transient receptor potential canonical channels induces the translation and synaptic incorporation of GluA1-containing calcium-permeable AMPA receptors. J Neurosci 32:8127-8137.

Geiger JR, Lubke J, Roth A, Frotscher M, Jonas P (1997) Submillisecond AMPA receptor-mediated signaling at a principal neuron-interneuron synapse. Neuron 18:1009-1023.

Geiger JR, Melcher T, Koh DS, Sakmann B, Seeburg PH, Jonas P, Monyer H (1995) Relative abundance of subunit mRNAs determines gating and Ca2+ permeability of AMPA receptors in principal neurons and interneurons in rat CNS. Neuron 15:193-204.

Ghosh A, Ginty DD, Bading H, Greenberg ME (1994) Calcium regulation of gene expression in neuronal cells. J Neurobiol 25:294-303.

Gomperts SN, Carroll R, Malenka RC, Nicoll RA (2000) Distinct roles for ionotropic and metabotropic glutamate receptors in the maturation of excitatory synapses. J Neurosci 20:2229-2237.

Goodman LJ, Valverde J, Lim F, Geschwind MD, Federoff HJ, Geller AI, Hefti F (1996) Regulated release and polarized localization of brain-derived neurotrophic factor in hippocampal neurons. Mol Cell Neurosci 7:222-238.

Grantyn R, Henneberger C, Juttner R, Meier JC, Kirischuk S (2011) Functional hallmarks of GABAergic synapse maturation and the diverse roles of neurotrophins. Front Cell Neurosci 5:13.

Greenberg ME, Hermanowski AL, Ziff EB (1986) Effect of protein synthesis inhibitors on growth factor activation of c-fos, c-myc, and actin gene transcription. Mol Cell Biol 6:1050-1057.

Gulyas AI, Gorcs TJ, Freund TF (1990) Innervation of different peptide-containing neurons in the hippocampus by GABAergic septal afferents. Neuroscience 37:31-44.

Guy J, Hendrich B, Holmes M, Martin JE, Bird A (2001) A mouse Mecp2-null mutation causes neurological symptoms that mimic Rett syndrome. Nat Genet 27:322-326.

Han ZS, Buhl EH, Lorinczi Z, Somogyi P (1993) A high degree of spatial selectivity in the axonal and dendritic domains of physiologically identified local-circuit neurons in the dentate gyrus of the rat hippocampus. Eur J Neurosci 5:395-410.

Harms KJ, Tovar KR, Craig AM (2005) Synapse-specific regulation of AMPA receptor subunit composition by activity. J Neurosci 25:6379-6388.

Hartman KN, Pal SK, Burrone J, Murthy VN (2006) Activity-dependent regulation of inhibitory synaptic transmission in hippocampal neurons. Nat Neurosci 9:642-649.

Hollmann M, Heinemann S (1994) Cloned glutamate receptors. Annu Rev Neurosci 17:31-108.

Isa T, Itazawa S, Iino M, Tsuzuki K, Ozawa S (1996) Distribution of neurones expressing inwardly rectifying and Ca(2+)-permeable AMPA receptors in rat hippocampal slices. J Physiol 491 (Pt 3):719-733.

Jiang B, Huang ZJ, Morales B, Kirkwood A (2005) Maturation of GABAergic transmission and the timing of plasticity in visual cortex. Brain Res Brain Res Rev 50:126-133.

Jonas P, Burnashev N (1995) Molecular mechanisms controlling calcium entry through AMPA-type glutamate receptor channels. Neuron 15:987-990.

Jonas P, Racca C, Sakmann B, Seeburg PH, Monyer H (1994) Differences in Ca2+ permeability of AMPA-type glutamate receptor channels in neocortical neurons caused by differential GluR-B subunit expression. Neuron 12:1281-1289.
Katz LC, Shatz CJ (1996) Synaptic activity and the construction of cortical circuits. Science 274:1133-1138.
Kandel ER, Siegelbaum SA (2000) Chapter 10 Overview of synaptic transmission, in Principle of Neural Science, 4th edition (Kandel ER, Schwartz JH, Jessell TM ed) McGraw-Hill, New York, pp 175-186.
Kim JH, Lee SR, Li LH, Park HJ, Park JH, Lee KY, Kim MK, Shin BA, Choi SY (2011) High cleavage efficiency of a 2A peptide derived from porcine teschovirus-1 in human cell lines, zebrafish and mice. PLoS One 6:e18556.
Kirischuk S, Juttner R, Grantyn R (2005) Time-matched pre- and postsynaptic changes of GABAergic synaptic transmission in the developing mouse superior colliculus. J Physiol 563:795-807.
Klausberger T, Somogyi P (2008) Neuronal diversity and temporal dynamics: the unity of hippocampal circuit operations. Science 321:53-57.
Kleschevnikov AM, Belichenko PV, Faizi M, Jacobs LF, Htun K, Shamloo M, Mobley WC (2012) Deficits in cognition and synaptic plasticity in a mouse model of Down syndrome ameliorated by GABAB receptor antagonists. J Neurosci 32:9217-9227.
Knight ZA, Tan K, Birsoy K, Schmidt S, Garrison JL, Wysocki RW, Emiliano A, Ekstrand MI, Friedman JM (2012) Molecular profiling of activated neurons by phosphorylated ribosome capture. Cell 151:1126-1137.
Koester HJ, Johnston D (2005) Target cell-dependent normalization of transmitter release at neocortical synapses. Science 308:863-866.
Kuzirian MS, Paradis S (2011) Emerging themes in GABAergic synapse development. Prog Neurobiol 95:68-87.
Liu SQ, Cull-Candy SG (2000) Synaptic activity at calcium-permeable AMPA receptors induces a switch in receptor subtype. Nature 405:454-458.
Lois C, Hong EJ, Pease S, Brown EJ, Baltimore D (2002) Germline transmission and tissue-specific expression of transgenes delivered by lentiviral vectors. Science 295:868-872.
Lu B, Wang KH, Nose A (2009) Molecular mechanisms underlying neural circuit formation. Curr Opin Neurobiol 19:162-167.
Malinow R, Malenka RC (2002) AMPA receptor trafficking and synaptic plasticity. Annu Rev Neurosci 25:103-126.
Mann EO, Paulsen O (2007) Role of GABAergic inhibition in hippocampal network oscillations. Trends Neurosci 30:343-349.
Marty S, Wehrle R, Sotelo C (2000) Neuronal activity and brain-derived neurotrophic factor regulate the density of inhibitory synapses in organotypic slice cultures of postnatal hippocampus. J Neurosci 20:8087-8095.
Marty S, Wehrle R, Fritschy JM, Sotelo C (2004) Quantitative effects produced by modifications of neuronal activity on the size of GABAA receptor clusters in hippocampal slice cultures. Eur J Neurosci 20:427-440.
Matarazzo V, Cohen D, Palmer AM, Simpson PJ, Khokhar B, Pan SJ, Ronnett GV (2004) The transcriptional repressor Mecp2 regulates terminal neuronal differentiation. Mol Cell Neurosci 27:44-58.

McBain CJ, Dingledine R (1993) Heterogeneity of synaptic glutamate receptors on CA3 stratum radiatum interneurones of rat hippocampus. J Physiol 462:373-392.
Mennerick S, Que J, Benz A, Zorumski CF (1995) Passive and synaptic properties of hippocampal neurons grown in microcultures and in mass cultures. J Neurophysiol 73:320-332.
Meyuhas O (2008) Physiological roles of ribosomal protein S6: one of its kind. Int Rev Cell Mol Biol 268:1-37.
Mitra A, Mitra SS, Tsien RW (2012) Heterogeneous reallocation of presynaptic efficacy in recurrent excitatory circuits adapting to inactivity. Nat Neurosci 15:250-257.
Morales B, Choi SY, Kirkwood A (2002) Dark rearing alters the development of GABAergic transmission in visual cortex. J Neurosci 22:8084-8090.
Morgan JI, Curran T (1991) Stimulus-transcription coupling in the nervous system: involvement of the inducible proto-oncogenes fos and jun. Annu Rev Neurosci 14:421-451.
Murthy VN, Schikorski T, Stevens CF, Zhu Y (2001) Inactivity produces increases in neurotransmitter release and synapse size. Neuron 32:673-682.
Nakata H, Nakamura S (2007) Brain-derived neurotrophic factor regulates AMPA receptor trafficking to post-synaptic densities via IP3R and TRPC calcium signaling. FEBS Lett 581:2047-2054.
Neher E, Sakaba T (2008) Multiple roles of calcium ions in the regulation of neurotransmitter release. Neuron 59:861-872.
Noebels JL (2003) The biology of epilepsy genes. Annu Rev Neurosci 26:599-625.
Nuber UA, Kriaucionis S, Roloff TC, Guy J, Selfridge J, Steinhoff C, Schulz R, Lipkowitz B, Ropers HH, Holmes MC, Bird A (2005) Up-regulation of glucocorticoid-regulated genes in a mouse model of Rett syndrome. Hum Mol Genet 14:2247-2256.
Oheim M, Kirchhoff F, Stuhmer W (2006) Calcium microdomains in regulated exocytosis. Cell Calcium 40:423-439.
Palizvan MR, Sohya K, Kohara K, Maruyama A, Yasuda H, Kimura F, Tsumoto T (2004) Brain-derived neurotrophic factor increases inhibitory synapses, revealed in solitary neurons cultured from rat visual cortex. Neuroscience 126:955-966.
Paradis S, Sweeney ST, Davis GW (2001) Homeostatic control of presynaptic release is triggered by postsynaptic membrane depolarization. Neuron 30:737-749.
Park H, Poo MM (2013) Neurotrophin regulation of neural circuit development and function. Nat Rev Neurosci 14:7-23.
Pelkey KA, McBain CJ (2008) Target-cell-dependent plasticity within the mossy fibre-CA3 circuit reveals compartmentalized regulation of presynaptic function at divergent release sites. J Physiol 586:1495-1502.
Platt SR (2007) The role of glutamate in central nervous system health and disease--a review. Vet J 173:278-286.
Pozo K, Goda Y (2010) Unraveling mechanisms of homeostatic synaptic plasticity. Neuron 66:337-351.
Pratt KG, Aizenman CD (2007) Homeostatic regulation of intrinsic excitability and synaptic transmission in a developing visual circuit. J Neurosci 27:8268-8277.

Racca C, Catania MV, Monyer H, Sakmann B (1996) Expression of AMPA-glutamate receptor B subunit in rat hippocampal GABAergic neurons. Eur J Neurosci 8:1580-1590.
Rao A, Craig AM (1997) Activity regulates the synaptic localization of the NMDA receptor in hippocampal neurons. Neuron 19:801-812.
Reyes A, Lujan R, Rozov A, Burnashev N, Somogyi P, Sakmann B (1998) Target-cell-specific facilitation and depression in neocortical circuits. Nat Neurosci 1:279-285.
Rizzoli SO, Betz WJ (2005) Synaptic vesicle pools. Nat Rev Neurosci 6:57-69.
Rosenmund C, Stevens CF (1996) Definition of the readily releasable pool of vesicles at hippocampal synapses. Neuron 16:1197-1207.
Rubenstein JL, Merzenich MM (2003) Model of autism: increased ratio of excitation/inhibition in key neural systems. Genes Brain Behav 2:255-267.
Rutherford LC, DeWan A, Lauer HM, Turrigiano GG (1997) Brain-derived neurotrophic factor mediates the activity-dependent regulation of inhibition in neocortical cultures. J Neurosci 17:4527-4535.
Schneggenburger R, Meyer AC, Neher E (1999) Released fraction and total size of a pool of immediately available transmitter quanta at a calyx synapse. Neuron 23:399-409.
Shen W, McKeown CR, Demas JA, Cline HT (2011) Inhibition to excitation ratio regulates visual system responses and behavior in vivo. J Neurophysiol 106:2285-2302.
Shigemoto R, Kulik A, Roberts JD, Ohishi H, Nusser Z, Kaneko T, Somogyi P (1996) Target-cell-specific concentration of a metabotropic glutamate receptor in the presynaptic active zone. Nature 381:523-525.
Sohal VS, Zhang F, Yizhar O, Deisseroth K (2009) Parvalbumin neurons and gamma rhythms enhance cortical circuit performance. Nature 459:698-702.

Stevens CF, Tsujimoto T (1995) Estimates for the pool size of releasable quanta at a single central synapse and for the time required to refill the pool. Proc Natl Acad Sci U S A 92:846-849.
Stevens CF, Williams JH (2007) Discharge of the readily releasable pool with action potentials at hippocampal synapses. J Neurophysiol 98:3221-3229.
Sun HY, Lyons SA, Dobrunz LE (2005) Mechanisms of target-cell specific short-term plasticity at Schaffer collateral synapses onto interneurones versus pyramidal cells in juvenile rats. J Physiol 568:815-840.
Tamamaki N, Yanagawa Y, Tomioka R, Miyazaki J, Obata K, Kaneko T (2003) Green fluorescent protein expression and colocalization with calretinin, parvalbumin, and somatostatin in the GAD67-GFP knock-in mouse. J Comp Neurol 467:60-79.
Tang AH, Chai Z, Wang SQ (2007) Dark rearing alters the short-term synaptic plasticity in visual cortex. Neurosci Lett 422:49-53.
Thiagarajan TC, Lindskog M, Tsien RW (2005) Adaptation to synaptic inactivity in hippocampal neurons. Neuron 47:725-737.
Thomson AM (1997) Activity-dependent properties of synaptic transmission at two classes of connections made by rat neocortical pyramidal axons in vitro. J Physiol 502 (Pt 1):131-147.

Traynelis SF, Wollmuth LP, McBain CJ, Menniti FS, Vance KM, Ogden KK, Hansen KB, Yuan H, Myers SJ, Dingledine R (2010) Glutamate receptor ion channels: structure, regulation, and function. Pharmacol Rev 62:405-496.

Tropea D, Giacometti E, Wilson NR, Beard C, McCurry C, Fu DD, Flannery R, Jaenisch R, Sur M (2009) Partial reversal of Rett Syndrome-like symptoms in MeCP2 mutant mice. Proc Natl Acad Sci U S A 106:2029-2034.

Turrigiano G (2007) Homeostatic signaling: the positive side of negative feedback. Curr Opin Neurobiol 17:318-324.

Turrigiano GG (2008) The self-tuning neuron: synaptic scaling of excitatory synapses. Cell 135:422-435.

Turrigiano GG, Nelson SB (2000) Hebb and homeostasis in neuronal plasticity. Curr Opin Neurobiol 10:358-364.

Turrigiano GG, Nelson SB (2004) Homeostatic plasticity in the developing nervous system. Nat Rev Neurosci 5:97-107.

Varoqueaux F, Sigler A, Rhee JS, Brose N, Enk C, Reim K, Rosenmund C (2002) Total arrest of spontaneous and evoked synaptic transmission but normal synaptogenesis in the absence of Munc13-mediated vesicle priming. Proc Natl Acad Sci U S A 99:9037-9042.

Verhage M, Maia AS, Plomp JJ, Brussaard AB, Heeroma JH, Vermeer H, Toonen RF, Hammer RE, van den Berg TK, Missler M, Geuze HJ, Sudhof TC (2000) Synaptic assembly of the brain in the absence of neurotransmitter secretion. Science 287:864-869.

Vicario-Abejon C, Collin C, McKay RD, Segal M (1998) Neurotrophins induce formation of functional excitatory and inhibitory synapses between cultured hippocampal neurons. J Neurosci 18:7256-7271.

Waites CL, Craig AM, Garner CC (2005) Mechanisms of vertebrate synaptogenesis. Annu Rev Neurosci 28:251-274.

Wierenga CJ, Ibata K, Turrigiano GG (2005) Postsynaptic expression of homeostatic plasticity at neocortical synapses. J Neurosci 25:2895-2905.

Wierenga CJ, Walsh MF, Turrigiano GG (2006) Temporal regulation of the expression locus of homeostatic plasticity. J Neurophysiol 96:2127-2133.

Wong WT, Wong RO (2001) Changing specificity of neurotransmitter regulation of rapid dendritic remodeling during synaptogenesis. Nat Neurosci 4:351-352.

Wood L, Gray NW, Zhou Z, Greenberg ME, Shepherd GM (2009) Synaptic circuit abnormalities of motor-frontal layer 2/3 pyramidal neurons in an RNA interference model of methyl-CpG-binding protein 2 deficiency. J Neurosci 29:12440-12448.

Xue M, Reim K, Chen X, Chao HT, Deng H, Rizo J, Brose N, Rosenmund C (2007) Distinct domains of complexin I differentially regulate neurotransmitter release. Nat Struct Mol Biol 14:949-958.

Yizhar O, Fenno LE, Prigge M, Schneider F, Davidson TJ, O'Shea DJ, Sohal VS, Goshen I, Finkelstein J, Paz JT, Stehfest K, Fudim R, Ramakrishnan C, Huguenard JR, Hegemann P, Deisseroth K (2011) Neocortical excitation/inhibition balance in information processing and social dysfunction. Nature 477:171-178.

Zhang ZW, Zak JD, Liu H (2010) MeCP2 is required for normal development of GABAergic circuits in the thalamus. J Neurophysiol 103:2470-2481.

Zhao C, Dreosti E, Lagnado L (2011) Homeostatic synaptic plasticity through changes in presynaptic calcium influx. J Neurosci 31:7492-7496.
Zoghbi HY (2003) Postnatal neurodevelopmental disorders: meeting at the synapse? Science 302:826-830.
Zucker RS, Regehr WG (2002) Short-term synaptic plasticity. Annu Rev Physiol 64:355-405.

Affidavit

“I, Chia-Ling Chang certify under penalty of perjury by my own signature that I have submitted the thesis on the topic: “The two-neuron microcircuit: An *in vitro* model for studying synapse formation and function”. I wrote this thesis independently and without assistance from third parties, I used no other aids than the listed sources and resources.

All points based literally or in spirit on publications or presentations of other authors are, as such, in proper citations (see "uniform requirements for manuscripts (URM)" the ICMJE www.icmje.org) indicated. The sections on methodology (in particular practical work, laboratory requirements, statistical processing) and results (in particular images, graphics and tables) correspond to the URM (s.o) and are answered by me. My interest in any publications to this dissertation corresponds to those that are specified in the following joint declaration with the responsible person and supervisor. All publications resulting from this thesis and which I am author correspond to the URM (see above) and I am solely responsible.

The importance of this affidavit and the criminal consequences of a false affidavit (section 156,161 of the Criminal Code) are known to me and I understand the rights and responsibilities stated therein.

Date Signature

Signature, date and stamp of the supervising University teacher

_____

Signature of the doctoral candidate

_____

"Mein Lebenslauf wird aus datenschutzrechtlichen Gründen in der elektronischen Version meiner Arbeit nicht veröffentlicht."

"Mein Lebenslauf wird aus datenschutzrechtlichen Gründen in der elektronischen Version meiner Arbeit nicht veröffentlicht."

Acknowledgement

I would like to thank to my supervisor Prof. Christian Rosenmund, for his great support and encouragement. During my PhD years, I learned not only the scientific knowledge but also the dedication to science from him. Most importantly, I thank him to give me the opportunity to experience two different cultures and countries during my PhD study.

I also would like to thank to all the colleague in the Rosenmund lab, especially to Thorsten and Melissa for working with the manuscript; Marcial, Marife and Tanja for help with the lab moving over sea; Johannes, Julia, Yuan-Ju, Ranjita, Charanya, Benjamin, Katharina, Gülçin and Frauke for all kinds of help. I thank Annegret, Sabine, Katja, Berit, Bettina, Hui-Deng, Hongmei for their excellent technical supports.

I like to thank to my previous graduate school, Baylor college of Medicine and Neuroscience program, also to the SFB 665 and Charité Graduate School GRK1123 for funding. Furthermore, I thank to Medical Neuroscience program of Charité - Universitätsmedizin Berlin.

Finally, I would like to thank to all my dear friends, especially to Sabrina and Karen. Most importantly, I want thank to my family, dear mom, dad, brother and 威宇's company and trust throughout my PhD years.